WP PWIE: SP D Reporting 2024

Andreas Kirschner & SP D task holders

This work has been carried out within the framework of the EUROfusion Consortium, funded by the European Union via the Euratom Research and Training Programme (Grant Agreement No 101052200 — EUROfusion). Views and opinions expressed are however those of the author(s) only and do not necessarily reflect those of the European Union or the European Commission. Neither the European Union nor the European Commission can be held responsible for them.

SP D Deliverables 2024

SP D.1 Plasma Boundary Modelling

D001: Plasma background parameters of WEST for modelling of impurity migration experiments (focus on long-pulse, high fluence discharges). **(CEA) 2PM**

D002: Plasma background parameters of linear devices (MAGNUM-PSI and UPP) for modelling of impurity migration experiments. **(DIFFER) 2PM**

D003: Plasma background parameters of GyM for modelling of impurity migration experiments (including He and Ar plasmas, validation against experiments under SP B). **(ENEA) 2PM**

D004: Plasma background parameters of W7-X and linear device PSI-2 for modelling of impurity migration experiments. **(FZJ) 4PM**

D005: PIC modelling to characterize the sheath with focus on W (prompt) redeposition studies. **(IPP.CR) 5PM**

D006: Plasma background parameters for JET-ILW for modelling of impurity migration experiments, focus on JET-ILW (e.g. prompt W redeposition experiments). **(VTT) 3PM**

SP D Deliverables 2024

SP D.2 Production of Atomic/Molecular and Surface Data

D001: Dust production model for anomalous events and detached divertor conditions, identification of possible dust formation mechanisms like nucleation in fusion-relevant plasmas. Connection to experimental data (e.g. dust studies in WEST). **(CEA) 2PM**

D002: Sputtering and reflection data for surface systems including boron (e.g. W-B, B-O, and other combinations also containing D), including seeding projectiles (e.g. Ar, Kr, Xe). Development of according interaction potentials. **(ÖAW) 3PM**

D003: Erosion information (SPRAY code, SDTrimSP-3D) of surfaces including morphology, roughness, with focus on realistic fuzz surfaces. Comparison to experiments (e.g. PSI-2) and MD results. **(ÖAW) 2PM**

D004: Modelling of tungsten gap melting and bridging including comparison to experiments (e.g. from AUG). **(VR) 6PM**

D005: Sputtering and reflection yields for surfaces including boron (W-B). Application of more advanced (accurate) (ML, AI) interaction potential for W and B sputtering/reflection modelling. **(VTT) 5PM**

D006: Erosion information of 2D/3D surfaces with focus on lattice effects, including dynamics, amorphisation and polycrystalline surfaces in comparison to experiments. **(MPG) 2PM**

SP D Deliverables 2024

SP D.3 Impurity Migration Modelling

D001: SOLEDGE3X-ERO2.0 simulations of tungsten transport in WEST, determination of main tungsten sources in WEST, comparison with spectroscopy and post-mortem data. One focus on long-pulse, high-fluence discharges and full 3D treatment (antennae, magnetic field ripple). **(CEA) 2PM**

D002: ERO2.0 simulations of dynamic morphology studies in GyM with Ar (see also SP B). Global ERO2.0 migration simulations in GyM, also for the design of diagnostics. ERO2.0 modelling of erosion/deposition experiments in AUG H-mode scenarios (connected to WP TE SOLPS modelling). **(ENEA) 5PM**

D003: ERO and ERO2.0 modelling of ^{13}C injection experiments (local and global) in comparison to post-mortem data in W7-X and steady-state simulations. ERO2.0 predictive modelling for full W environment in W7-X. ERO and ERO2.0 modelling of W prompt redeposition, in combination with sheath characteristics from PIC. Initial simulations of ITER with full-W plasma-facing components and Ne seeding. **(FZJ) 17PM**

D004: Predictive material migration in full-W ITER including B transport resulting from boronisation. **(MPG) 2PM**

D005: ERO2.0 simulations of AUG erosion and migration experiments in L-mode D plasma and comparison with experimental data and former ERO simulations. **(VTT) 4PM**

D006: Self-charging and adhesive force calculations for boron dust. **(VR) 5PM**

SP D Deliverables 2024

SP D.4 Neutral Particles Modelling

D001: DIVGAS modelling: effect of 3D poloidal and toroidal leakages for the baseline SN divertor case. Optional: W7-X. **(KIT) 9PM**

D002: Atomic and molecular fluxes to the wall surfaces (including divertor) in JET-ILW. **(VTT) 2PM**

(I) Deliverables added during the year:

SP D.5 Plasma Background and PWI Modelling for COMPASS-U

D001: SOLPS-ITER plasma backgrounds for COMPASS-U H-mode scenarios. Sheath characteristics from PIC simulations. **(IPP.CR) 12 PM**

D002: Supervision of ERO2.0 modelling. **(FZJ) 1PM**

D003: SOLEDGE3X plasma backgrounds in comparison to SOLPS-ITER. **(CEA) 3 PM**

Voluntary contribution w/o PM: *1D simulations of SOL interaction in different regimes of T and n (sheath limited, high recycling, detached) w/o impurity seeding. Comparison to fluid modelling with SOLEDGE code of IRFM collaborators.* ***(ENEA) 0PM***

SP D Deliverables 2024

(II) Tasks added during the year under SP D.2 D005:

Task 1: MD simulations of N reflection from WN surfaces, including N2 molecular yield from fast processes. Impact energies below threshold for sputtering W atoms. Comparison to SDTrimSP.
(VTT / Aalto U) 1PM

Task 2: MD simulations of reflection and molecular sputtering yields from H/D/T-saturated W surfaces.
(VTT / Aalto U) 2PM

SP D.1 Plasma Boundary Modelling

G. Ciraolo

D001

SOLEDGE modeling for WEST plasma background (focus on long-pulse, high fluence discharges)

- WEST shot #58245 of the C7 high-fluence campaign

- SOLEDGE 2D transport axisymmetric simulations: scan in input power, separatrix density, impurity content,…

- Ongoing analysis on the impact of drifts on plasma profiles, in particular at the strike points

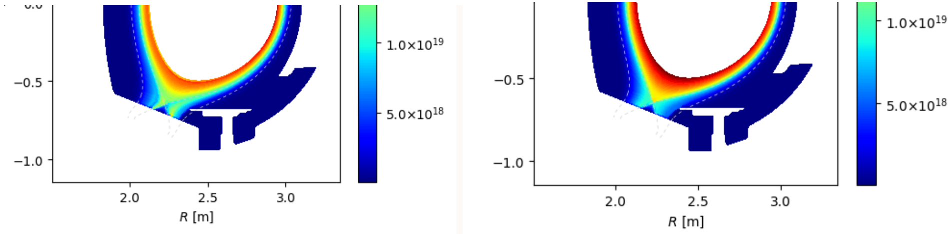

2D poloidal density map **w/wo drifts**

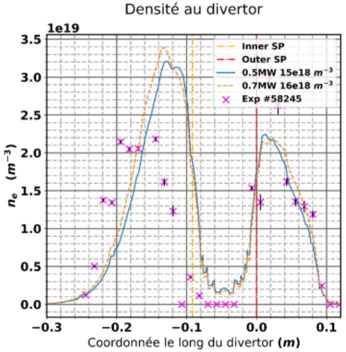

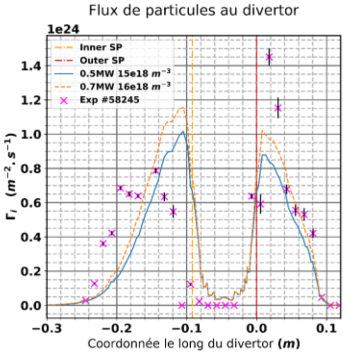

SOLEDGE3X modeling of WEST discharges taking into account magnetic ripple

G. Ciraolo

D001

- **3D WEST simulations with magnetic ripple obtained using the electromagnetic version of SOLEDGE**
- Set of relevant simulations for comparison with experimental data almost completed
- R. Dull et al, *Implementation of a non-axisymmetric magnetic configuration in SOLEDGE3X to simulate 3D toroidal magnetic ripple effects: Application to WEST*, accepted for publication in Nucl. Mat Ener.

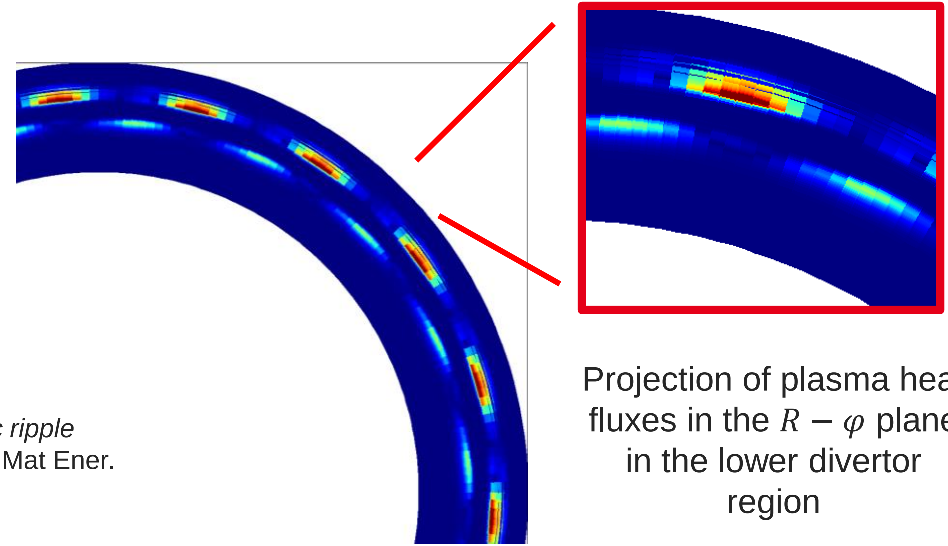

Projection of plasma heat fluxes in the $R-\varphi$ plane in the lower divertor region

→ **3D plasma backgrounds obtained for a set of input parameter**

→ **Ongoing analysis of the comparison with experimental data contamination**

SP D.1 Plasma Boundary Modelling: DIFFER

E. Westerhof,
H.J. de Blank

D002

SOLPS-ITER modelling of the plasma beam and vessel of MAGUM-PSI:

boundary condition for electric potential profile Φ(r) required

- To this end, line-integrated spectra of the Balmer-β emission in front of the plasma source are measured.
  - This radiation comes from excited H-atoms with a high CX-cross-section.
  - Therefore their Doppler shift corresponds to the ion rotation speed close to the location of emission.
  - The ion rotation speed in front of the plasma source is dominated by $v_{E\times B}$.
- In order to estimate $\Phi(r)$, the line-integrated spectra are decomposed into a hot co-rotating component inside the plasma beam and a cooler and slower component from the periphery.

An iteration step is made, adjusting the $\Phi(r)$ boundary condition such that the ion rotation speed at the lines of sight match the measurements.

SP D.1 Plasma Boundary Modelling: DIFFER

E. Westerhof,
H.J. de Blank

D002

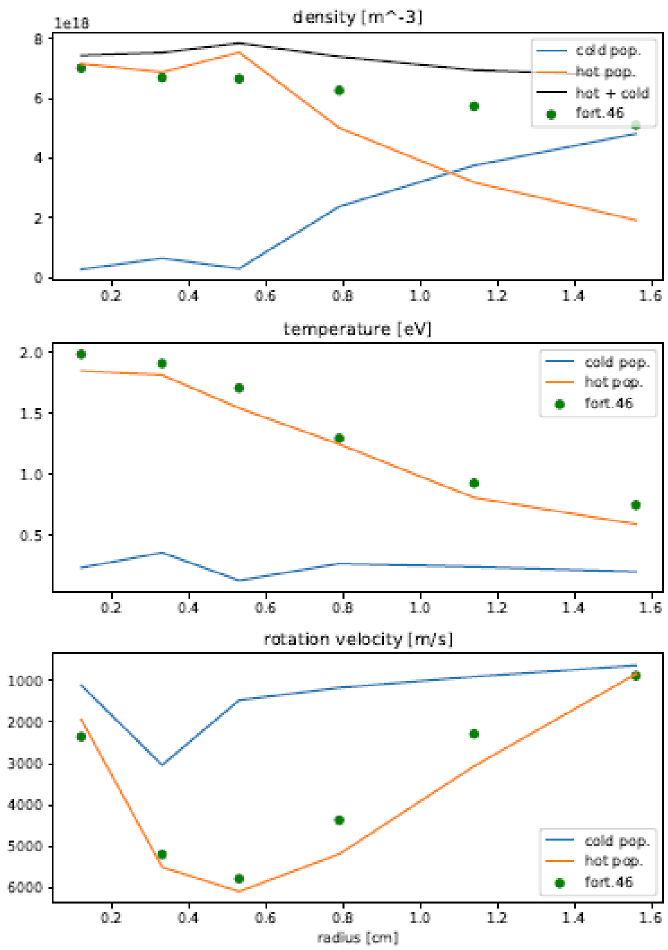

Analysis of directed spectra of the neutral velocity distributions in EIRENE:

a radially peaked profile of hot co-rotating H-atoms and a hollow profile of cooler non-rotating H-atoms.

Shown as dots: corresponding standard 1D-fluid Eirene quantities over all H-atoms.

SP D.1 Plasma Boundary Modelling: ENEA

M. Passoni

D003

SOLPS-ITER investigation of GyM He plasma

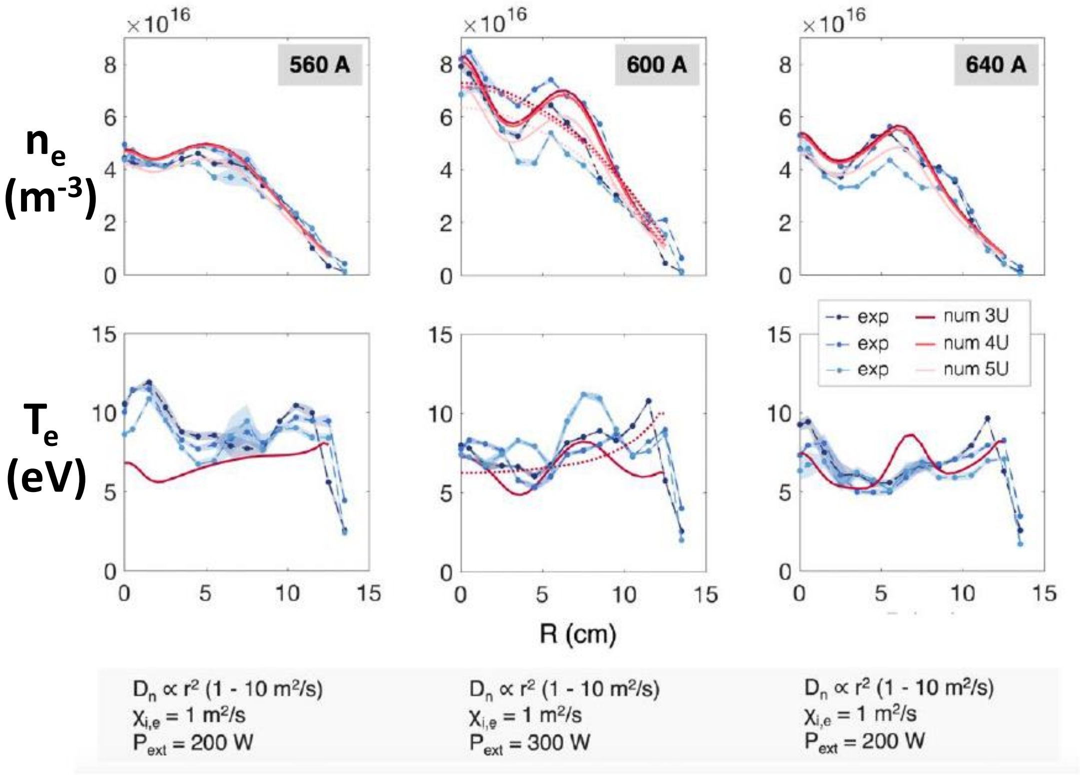

Validation of the numerical model against experimental data at different magnetic field configurations

- The electron density profiles have been identified as strongly correlated with the power absorbed by the plasma and vary across different magnetic field configurations.
- A plasma background for eventual erosion investigation (see SP D3) has been generated.

SP D.1 Plasma Boundary Modelling: ENEA

M. Passoni

D003

SOLPS-ITER investigation of GyM He plasma

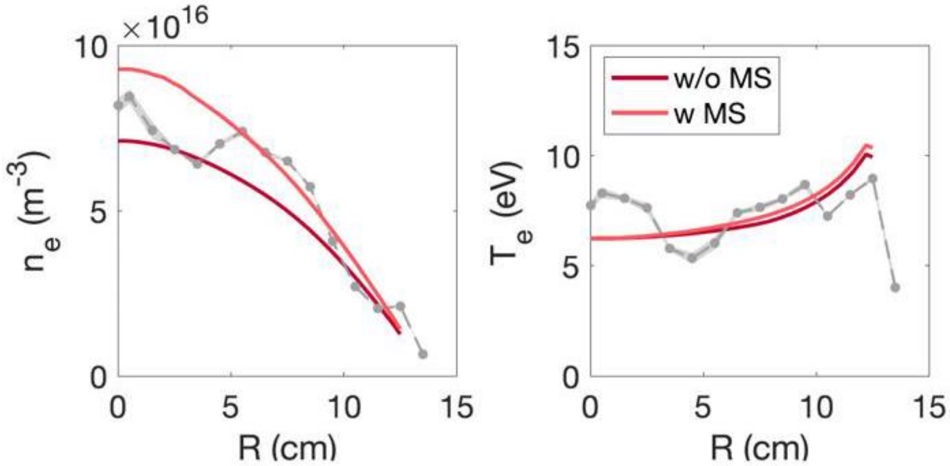

Inclusion of He metastable (MS) states among plasma neutral species

- The pre-existing difficulties in including metastable species among the neutral populations have been overcome.
- The addition of metastable species is accompanied by a noticeable increase in electron density. This is consistent, under certain assumptions, with the predictions of a previous 0D model for the GyM plasma

SP D.1 Plasma Boundary Modelling: ENEA

M. Passoni

D003

SOLPS-ITER investigation of GyM Ar plasma

- **Objective:** preliminary SOLPS numerical campaign supporting the interpretation of GyM Ar-plasma experiments to be performed in the framework of cross-machine comparison under SP B1.
- A set of preliminary simulations of Ar plasma has been conducted, investigating the role of various free parameters in the code through parametric scans, with a view toward subsequent validation work.

SP D.1 Plasma Boundary Modelling: FZJ

S. Xu

D004

Plasma background parameters of W7-X by EMC3-EIRENE

- Optimizing the EMC3-EIRENE calculation grid based on requirements of ERO2.0
- Providing EMC3-EIRENE simulations for ERO2.0 with/without plasma toroidal currents in standard configuration of W7-X

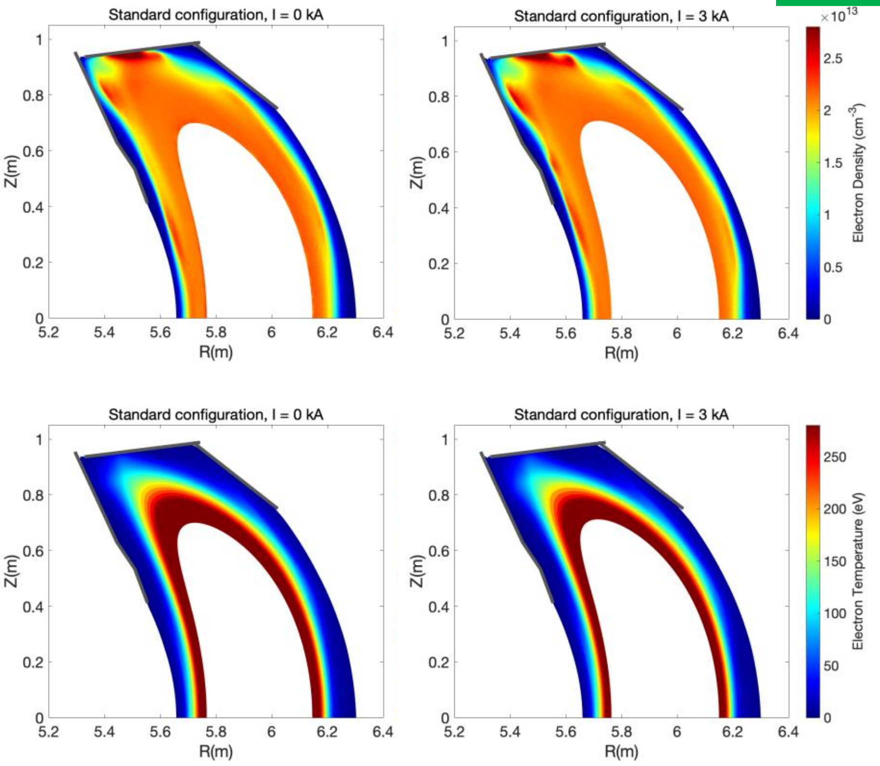

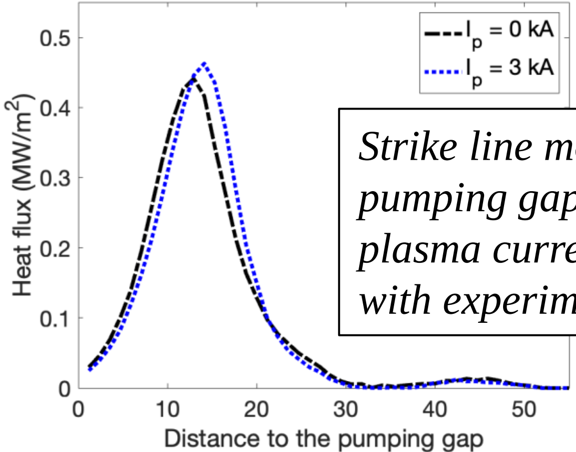

Strike line moves away from pumping gap with toroidal plasma current. (agreement with experiments)

Plasma background parameters of PSI-2 by SOLPS-ITER

D. Reiser

D004

- Installation of Code Package ✓
- Preparing Geometry Input ✓
- Test Run B2.5 Standalone ✓
- Preparing Visualization Tools ✓
- Preparing Source Input Files !
- Adjustment of Physics Parameters !
- B2.5 Standalone Runs !
- B2.5-Eirene Runs !

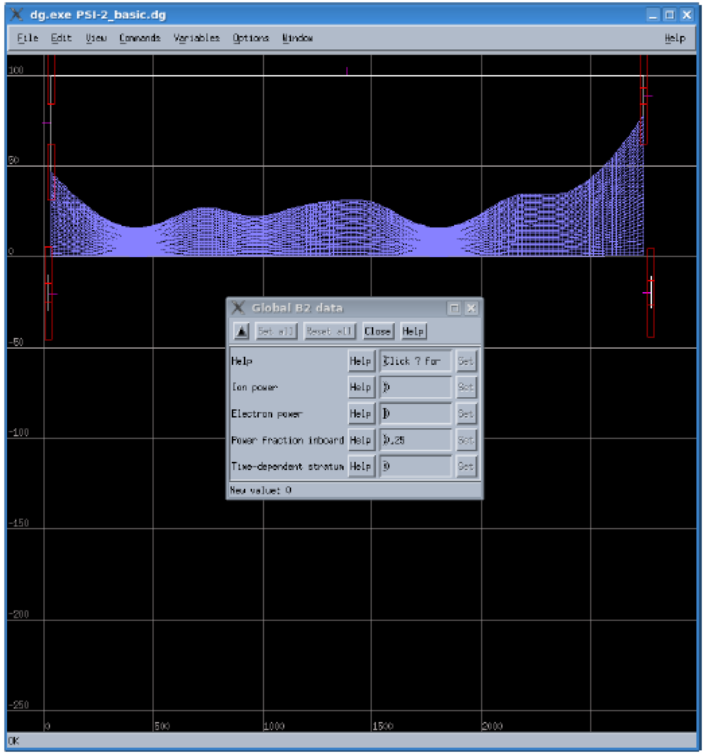

SP D.1 Plasma Boundary Modelling: IPP.CR

D. Tskhakaya

D005

BIT1 simulations of W sputtering

W recycling study in a high density divertor

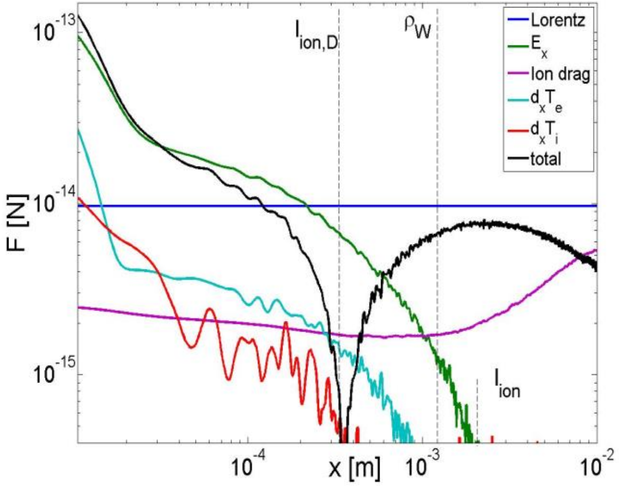

Forces acting on W^{+} ion in a high density divertor, $n_{e,\ sheath}$ = 6.9x10^{20} m^{-3} (PSI 2024).

- Due to reduction of the prompt re-deposition, **W sputtering** for high density cold divertor plasmas **should not be neglected** a-priory.
- For quantitative study access to a new **atomic data is required**, namely D+ + W CX and e + W ionization rates (derived from the CRM) .

ERO2.0 team was provided with DEMO relevant 1D divertor profiles

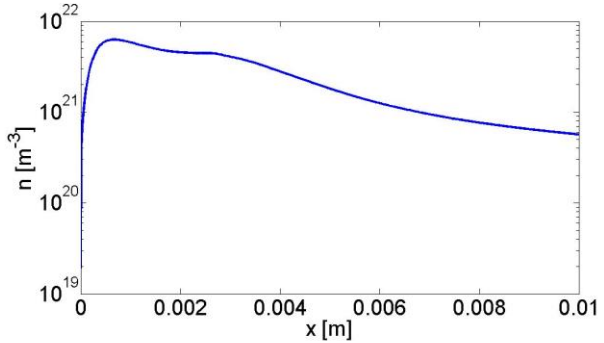

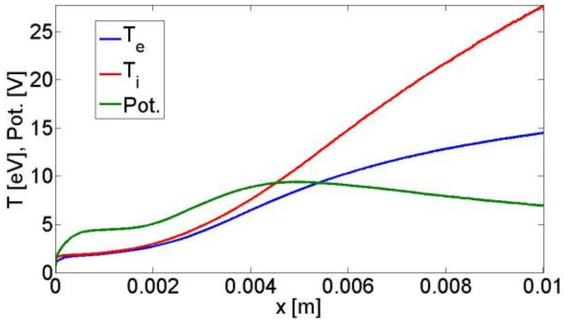

SP D.1 Plasma Boundary Modelling: IPP.CR

SPICE2 simulations of collisional boundary plasma

D. Tskhakaya, M. Komm

D005

- Studies of the influence of **charge exchange (CX) collisions** in plasmas with **high neutral density** and **hot emissive wall** on plasma sheath
- Closely linked the proposed regime of **inverse sheath**
- CX collision operator implemented, however some scenarios will require adjustments of the boundary conditions -> implementation of 2-wall scheme
- Observations so far: **CX causes trapping of cold ions** in the location of the virtual cathode (as predicted by inverse sheath theory). However, **Coulomb collisions (CC) cause ion de-trapping** so that the plasma does not switch to inverse sheath
- This pilot study needs to be extended to a wider parameter space -> more computational time needed

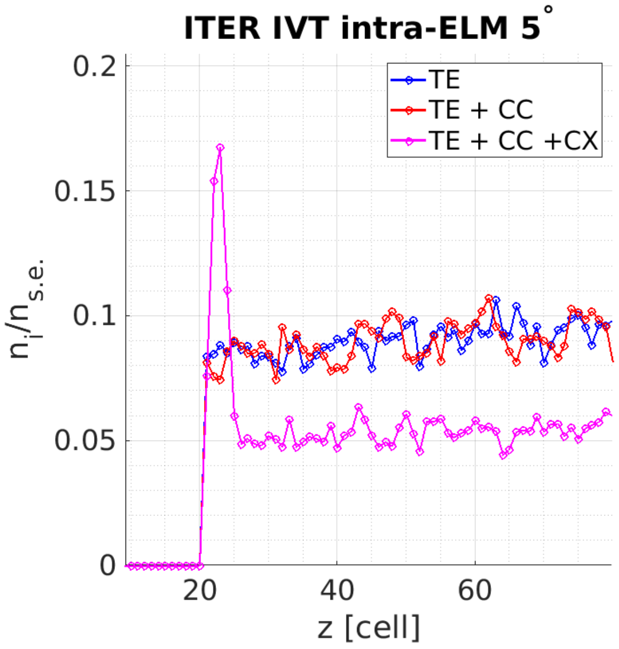

Comparison of ion density for hot emissive wall with no collisions (blue), Coulomb coll. (red) and CC with CX collisions (magenta)

SP D.1 Plasma Boundary Modelling: VTT / Aalto U

M. Groth

D006

SOLPS-ITER simulations of He vs D plasmas

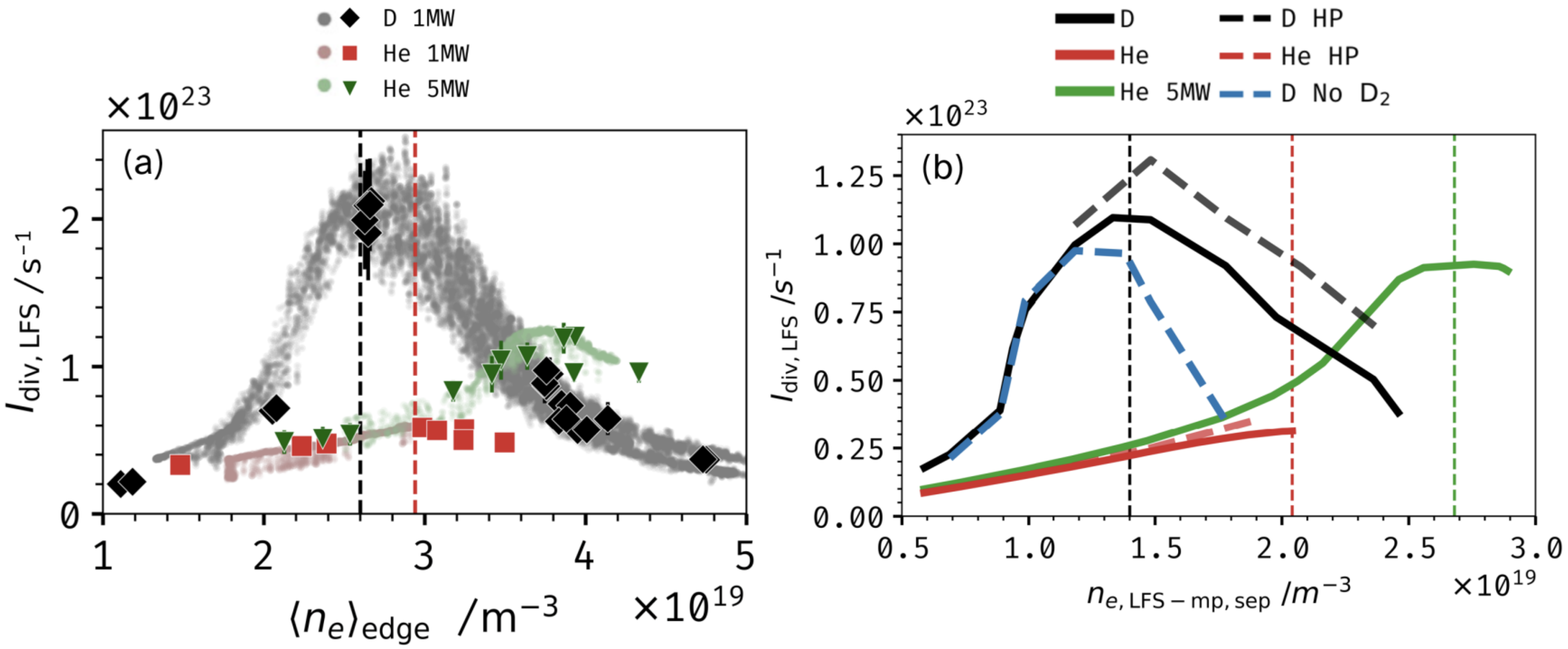

qualitatively consistent with measurements (70% lower $I_{div,LFS}$ in He) due to 1.5-3x higher eff. ionisation cost

SP D.1 Plasma Boundary Modelling: VTT / Aalto U

M. Groth

D006

JET limiter plasmas

LiPBaLM prediction for T_e

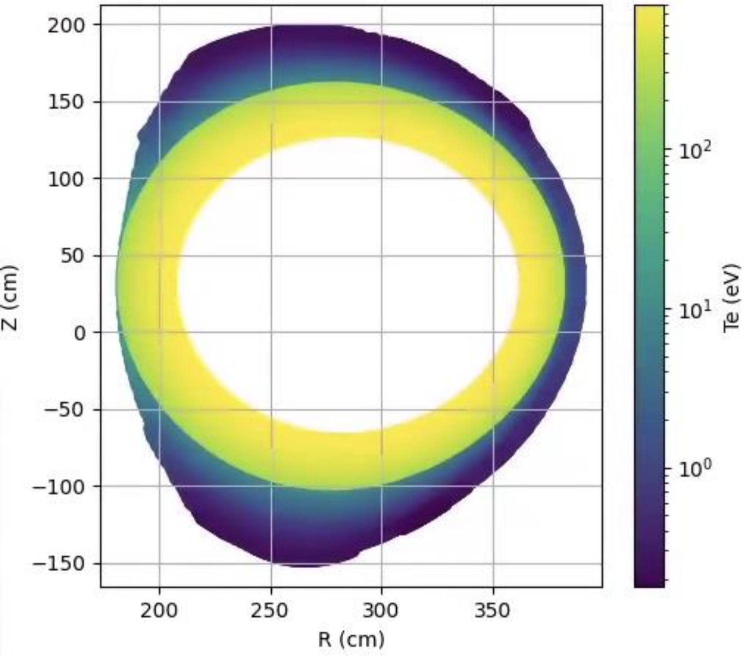

⇒

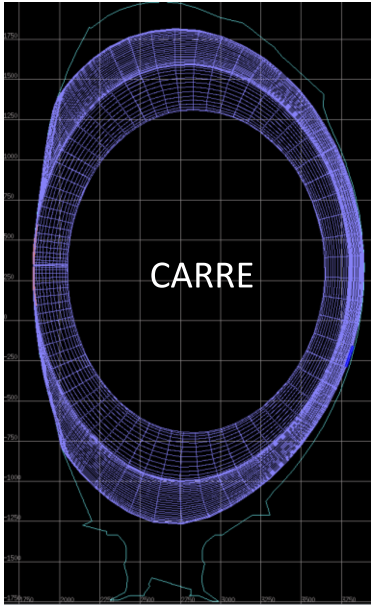

Simulated using a 2-PM/OSM (including internal grid generation)

⇒ CARRE grid for SOLPS-ITER (EIRENE CX fluxes)

SP D.1 Plasma Boundary Modelling: VTT / Aalto U

M. Groth

D006

Background plasma modelling for Ni & W migration modelling in JET

representative plasma configs. and scenarios in the JET-ILW campaigns 2011-2015

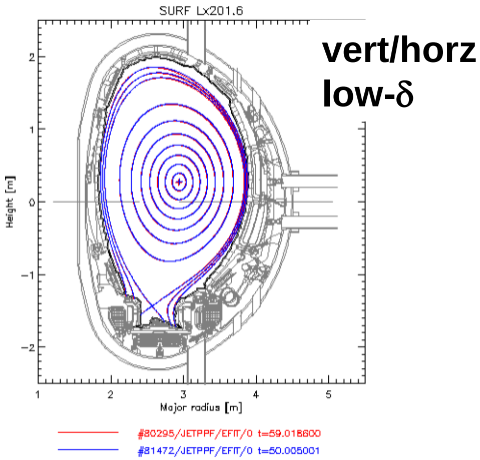

- Deuterium plasmas, EDGE2D-EIRENE density scan at low (2 MW) and moderate (up to 15 MW) heating power

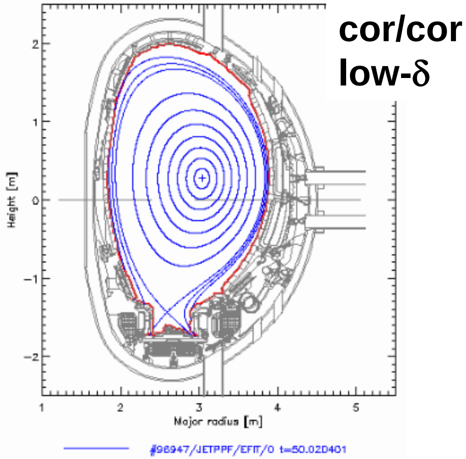

- Deuterium plasmas, JINTRAC (including EIRENE) density scan at low (2 MW) and high (up to 25 MW) heating power
- Inter and intra-ELM time slices for subset of density/power scans

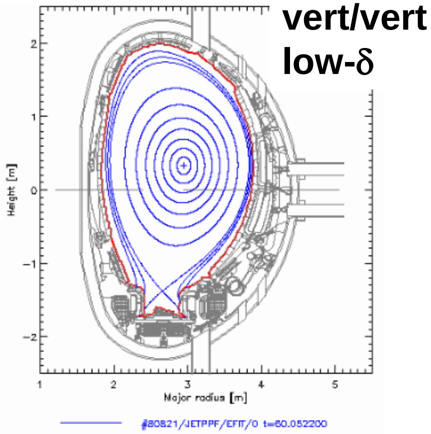

- Deuterium plasmas, EDGE2D-EIRENE density scan at low (2 MW) and moderate (up to 10 MW) heating power

SP D.2 Production of Atomic/Molecular and Surface Data

Nucleation process of tungsten nanoparticles

A. Michau

D001

Nucleation and growth in the equilibrium metal vapor after a thermal quench

Particle size distribtution evolutions after the nucleation burst

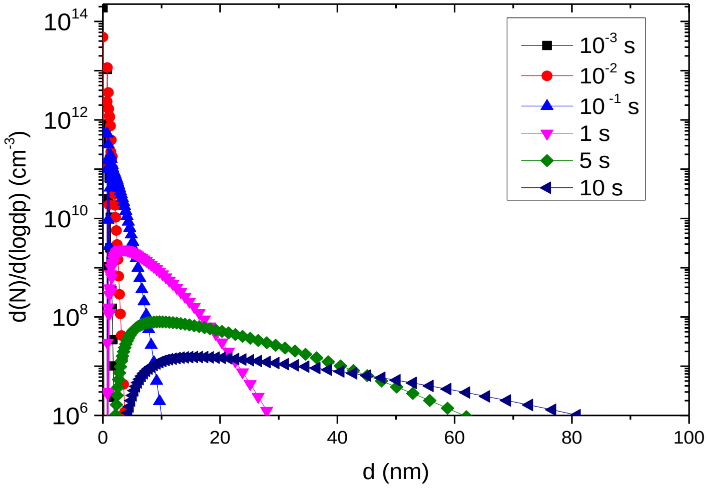

Coagulation ➔ decrease of the nucleus population ➔ formation of larger particles and a wide particle size-distribution

- A thermal quench of the equilibrium tungsten vapor (that may be produced or that surround a tungsten droplet emitted after after anomalous event) is simulated
- The nucleation inside the vapor is investigated
- Simulation conditions : T_0 = 4000 K, τ_{quench} =1 ms

A. Michau

D001

Nucleation process of tungsten nanoparticles

Investigation of nucleation through tungsten cluster growth

The objective is to obtain the cross section of cluster growth: $W_n^{0/+} + W \rightarrow W_{n+1}^{0/+}$

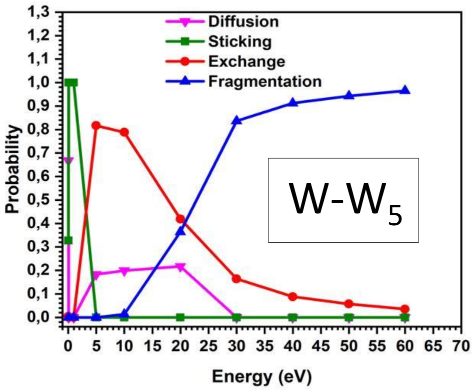

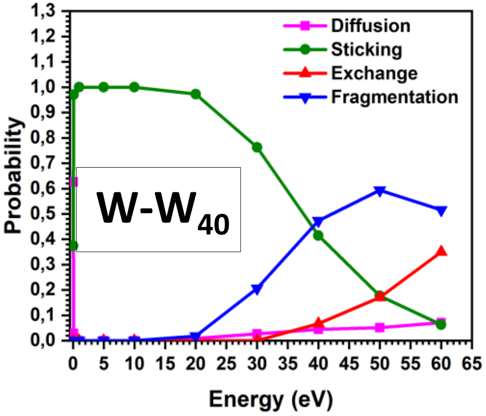

- The range of collision energy for which sticking and growth is possible increases with the cluster size
- The small clusters are the most difficult to produce

1) Sputtering yields of a B surface by D

M. Probst
S. Shermukhamedov

D002

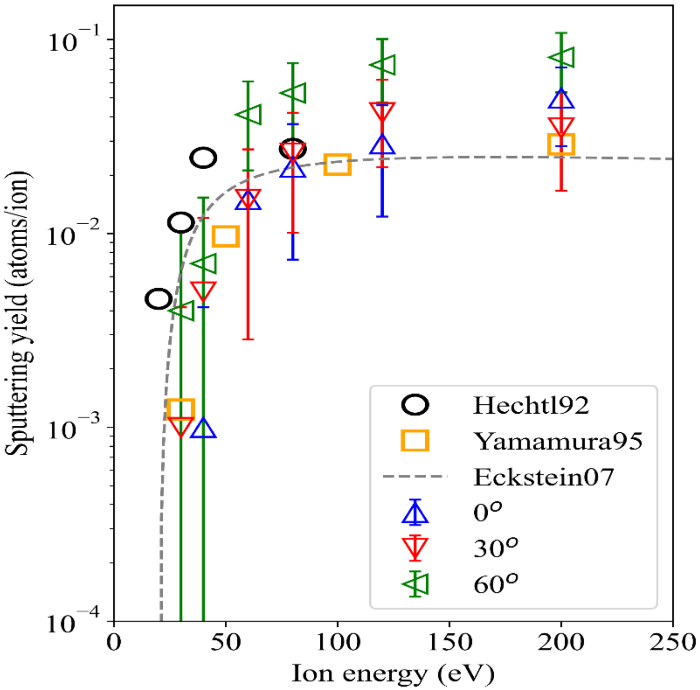

- We trained a Potential energy function of the Behler-Parrinello type for the B-D system and performed non-cumulative molecular dynamics simulations.
- The triangles show our sputtering yields for three different incident angles.
- Experimental data from Hechtl(1992) and theoretical data from Yamamura(1995), as well as the Eckstein curve (theoretical) are included.

SP D.2 Production of Atomic/Molecular and Surface Data: OEAW

M. Probst
S. Shermukhamedov

D002

2) Reflection/Adsorption/Retention probabilities of D in B

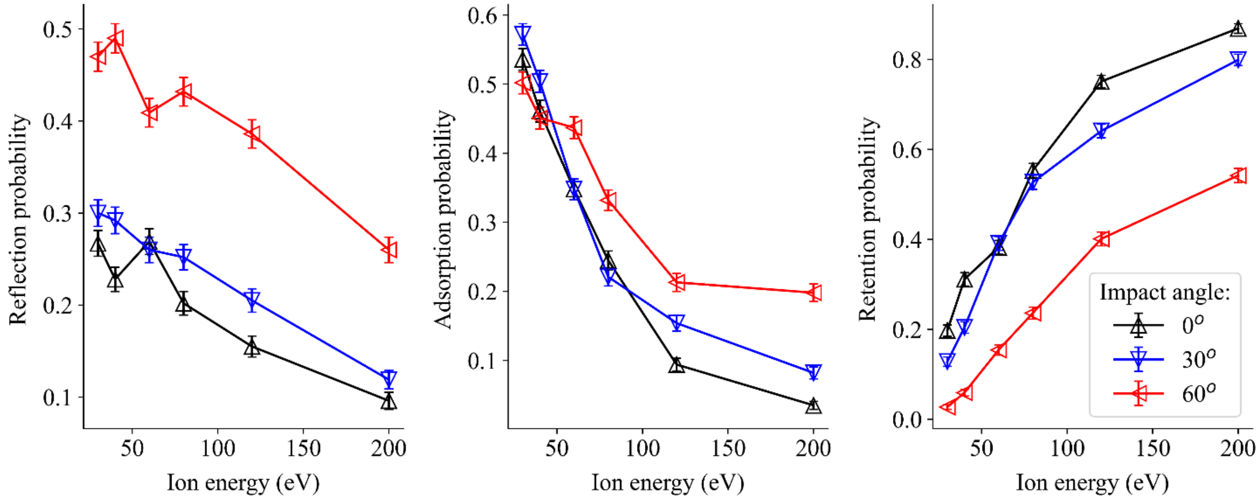

- At lower energies, reflection and adsorption compete, while at higher energies, retention prevails.
- Angular dependencies and surface binding energies were also analyzed.

- Also: boron self-sputtering has been studied

SP D.2 Production of Atomic/Molecular and Surface Data: OEAW

SDTrimSP-related modelling of erosion including morphology, roughness, fuzz (ÖAW)

F. Aumayr, J. Brötzner

D003

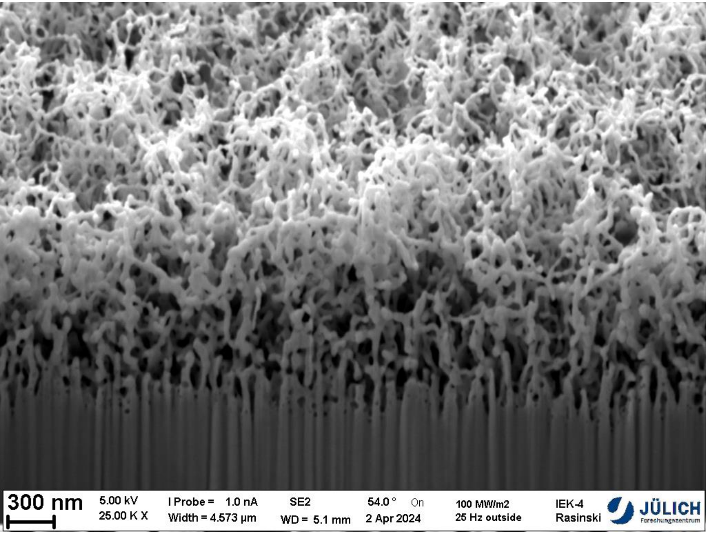

image of W fuzz,
© M. Rasinski

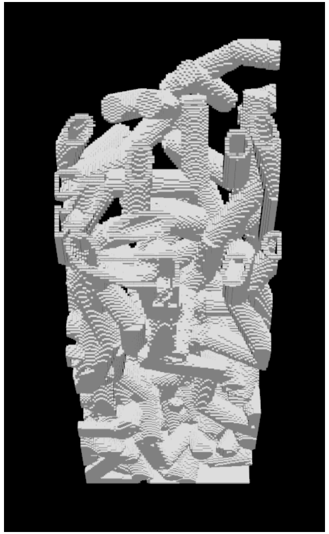

model used as input for SDTrimSP-3D, 100x100x 300 voxel corresponding to 500x500x1500 nm^3
Modelling algorithm adapter after [1]
(Tendrils are solid but appear hollow due to visualisation artifacts)

Dynamic simulations were carried out for the special case of 2 keV Ar at 60° to check for fluence dependent morphology and sputter yield changes.

[1] R. Stadlmayr et al., JNM 532 (2020) 152019

SP D.2 Production of Atomic/Molecular and Surface Data: OEAW

F. Aumayr, J. Brötzner

D003

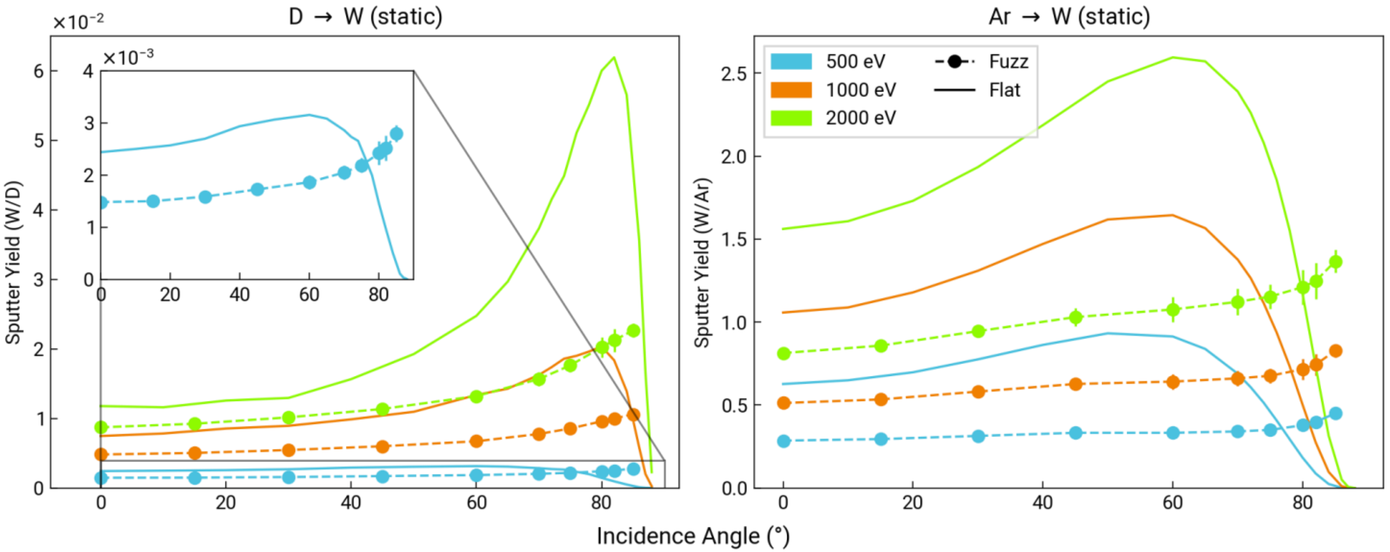

Results from static simulations: sputter yields over incidence angle for both flat surfaces and the fuzz structures shown on the previous slide.

The presence of fuzz leads to a significant reduction of the sputtering yield (both for D and Ar projectiles) and a flattening of its dependence on projectile incidence angle.

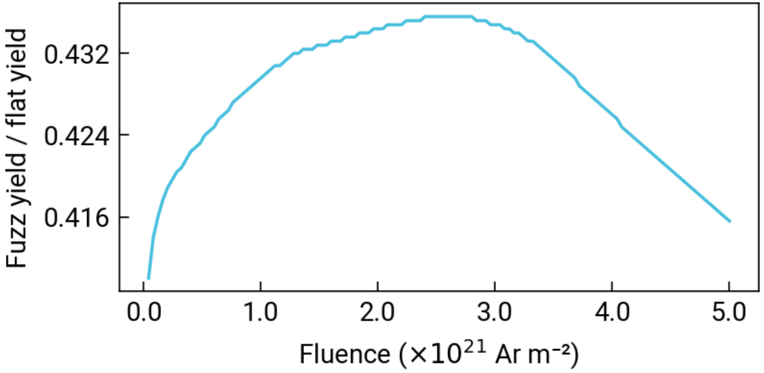

Preliminary results from first dynamic studies for 2 keV Ar under 60°; Simulations are still running, and from [1] one would expect a fluence of ~2e22 for similar fuzz thicknesses to be eroded. Simulations are expected to complete mid of November.

Gap melting simulations

S. Ratynskaia

D004

Objectives

- Validate melt dynamics simulations against experimental data on gap bridging/filling during high-energy events
- Explore sensitivity to input parameters (geometry, heat and current sources, etc)
- Extrapolate to ITER/DEMO scenarios

Simulated scenarios

W jetting across misaligned PFCs in AUG

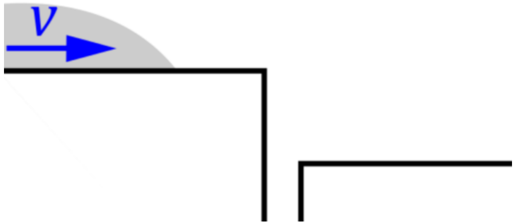

In-place Be castellation filling in JET

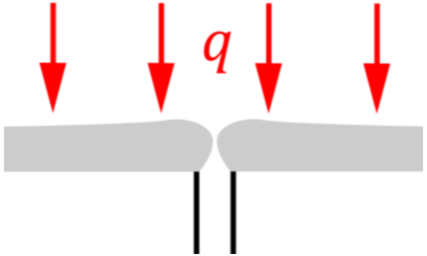

Main conclusions

- Experimental observations are successfully reproduced
- Previously obtained stability criteria for melt flows over sharp PFC edges are robust enough for extrapolation
- Cumulative deformations throughout multiple melt events can play a significant role in the bridging process

SP D.2 Production of Atomic/Molecular and Surface Data: VR

- Protruding W sample exposed to AUG ELMs [Krieger et al, *NF* 2018]
- **Melt created in the middle of the sample then moved to the 0.5 mm gap**
- **Four edge-crossing events** from MEMOS-U modelling [Ratynskaia et al, *NF* 2020] used as input for 2D simulations in Fluent
  - Independent runs: undamaged gap geometry enforced before each event
  - Sequential runs: morphology changes accumulate throughout

Results [pinboard #116286, submitted to *NF*]

- Dimensionless thresholds obtained from JET-relevant Be simulations [Vignitchouk et al, *NF* 2023] in terms of Weber number $\mathrm{We} = \rho h v^2/\gamma$ (inertia over surface tension) correctly predict flow stability in independent runs
- W mass crossing the gap agrees with measurements and increases with We
- Progressive rounding-off of the corner during sequential runs promotes better flow attachment, leading to gap bridging as in the experiment

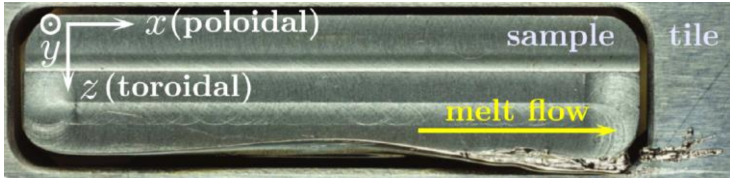

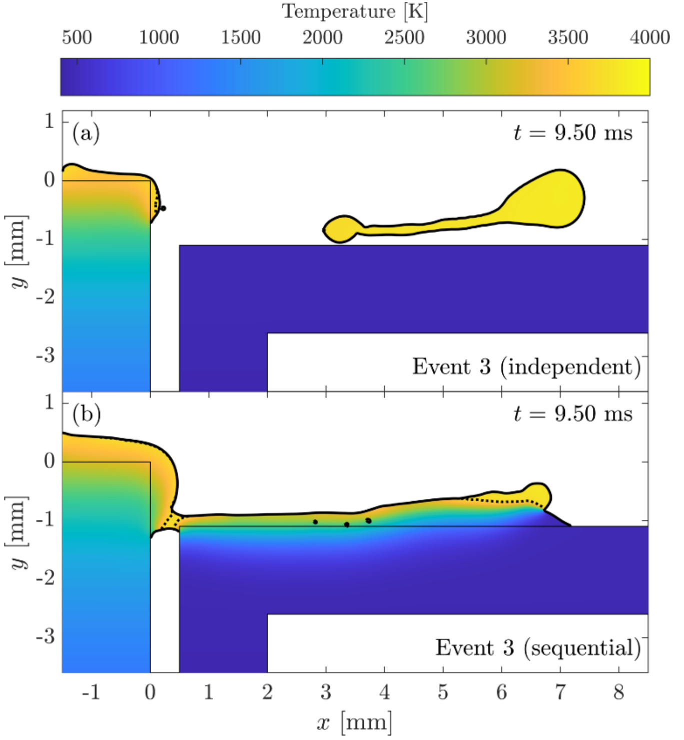

Top right: post-exposure photograph of the W sample

Right: comparison between independent and sequential runs of the event with the largest We

Bottom: growth of a re-solidified overhang and gap bridging in the sequential runs

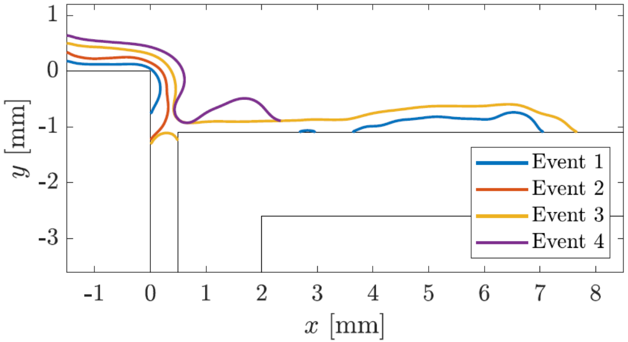

S. Ratynskaia D004

SP D.2 Production of Atomic/Molecular and Surface Data: VR

S. Ratynskaia

D004

- Be upper dump plate exposed to multiple JET CQs [Jepu et al, *NF* 2019]
- **Melt created uniformly on both sides of every 350 µm castellation and accelerated towards the low-field side**

Preliminary results

- Largest heat flux and $j \times B$ force values selected to simulate a **single, extreme CQ**
  - Uniform 500 MW/m^2 and 150 kN/m^3 loading (60 kA/m^2 halo current at 2.5 T magnetic field) during 35 ms
- Melt starts accumulating and bulging at the upstream gap edge before crossing can occur at ~ 25 ms
- The final re-solidified bridge is ~ 1 mm thick (experimental range: 0.2–3.5 mm)

Ongoing and planned work (completion foreseen early 2025)

- Repeat simulations with lower heat and momentum drives to assess influence on results and look for transition points
- Simulate a second CQ starting from the bridged geometry to test whether the fill depth increases

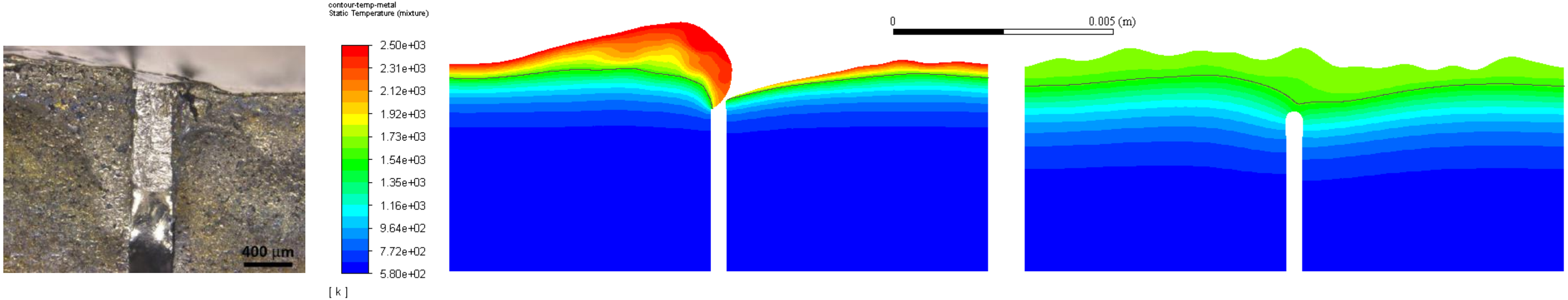

Left: photograph of a filled-in JET upper dump plate castellation. Middle and right: Fluent output just before bridging (t = 22.5 ms) and during the post CQ cool-down phase (t = 50 ms); the solid-liquid boundary is drawn in black.

SP D.2 Production of Atomic/Molecular and Surface Data: VTT

K. Nordlund / F. Granberg

D005

- Sputtering of W and D-decorated W surfaces, by Ar/Ne/W
  - Work is finished, conclusive data for pure W surfaces, inconclusive for D-decorated
    - Article on pristine sputtering being finished, to be submitted still 2024.
    - For D-decoration, opposite effect depending on interatomic potential. DFT verification ongoing.
    - None of existing classical potentials seems to be comparable to DFT.
    - To be continued in 2025. There is one ML potential to be published soon and our being developed (TSVV-7), both will be used to understand the D-decoration effect, and hopefully give a conclusive result.
- Sputtering of W by low and medium energy Ar ions finished
  - Low index, random and amorphous surfaces studied, both single and cumulative impacts
  - Sputtering yields and angular distributions are to be used and compared to higher scale models
  - Will be extended in 2025, according to needs found in higher scale models

SP D.2 Production of Atomic/Molecular and Surface Data: VTT

K. Nordlund / F. Granberg

D005

- Sputtering of W and W-based refractory high entropy alloys
  - To understand the effect of alloying on the sputtering, W and W-based HEAs have been studied
    - Preferential sputtering and depletion/increase of specific elements is observed on the surface by simulations. Most of the computational part is done, some parameter sets still running.
    - Experiments being designed to validate our preferential sputtering computational results
- W-B classical potential development, Tersoff-type, still ongoing by collaborators
  - No sputtering results yet, as the potential is not stable.
- W-B ML potential development
  - Will be developed once the ML W(-O-H) potential is verified for sputtering simulations

SP D.2 Production of Atomic/Molecular and Surface Data: VTT

A. Sand

D005

MD simulations of N reflection from WN surface

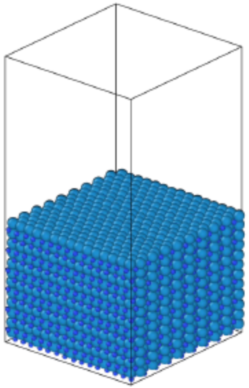

Simulation set-up:

- Non-cumulative bombardment of WN surface at 500 K
- 1:1 ratio of W and N
- NiAs crystal structure (lowest energy configuration of WN according to potential)
- Electronic stopping accounted for as friction force with magnitude predicted by SRIM
- Varying ion energy (1-100 eV) and impact angle (50,60,70 deg)

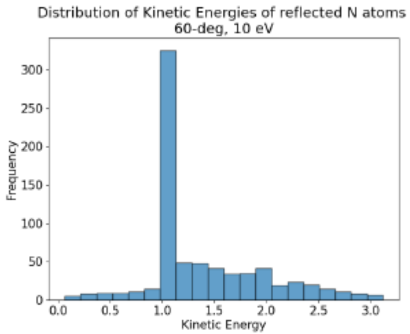

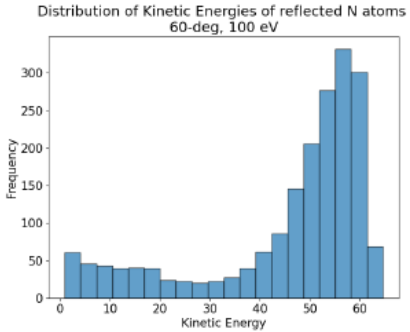

Statistics obtained for yields, and energies of sputtered and reflected species

- For higher impact energies and angles, reflected N retains high kinetic energy

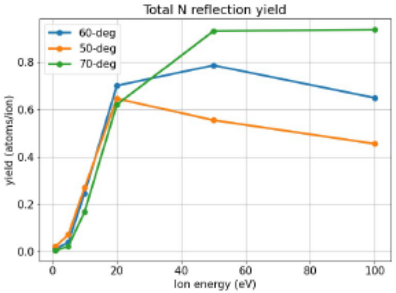

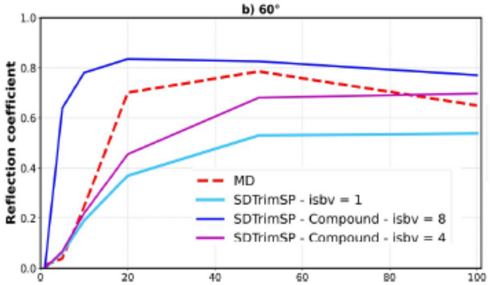

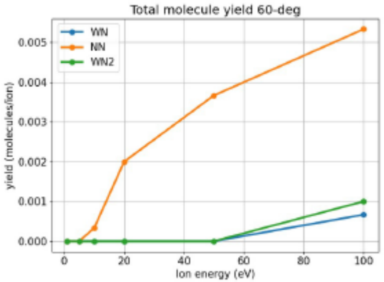

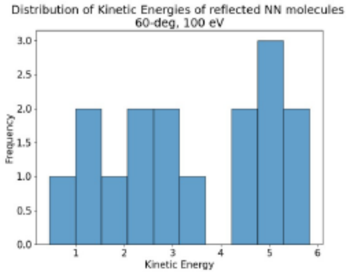

SP D.2 Production of Atomic/Molecular and Surface Data: VTT

A. Sand

D005

MD simulations of irradiation of H/D/T-saturated W surfaces

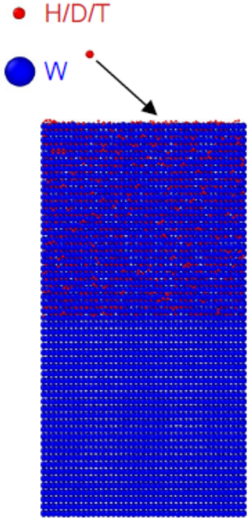

Goals:

- Modeling the reflection and molecular sputtering yields from the surface
- Providing some insight into the possible rotational-vibrational states of these sputtered molecules

MD simulations:

- Non-cumulative H/D/T bombardment of saturated W surfaces
- Cell equilibrated to 300 K and temperature maintained by border thermostat
- Varying ion impact energies
- Electronic stopping accounted for as friction force with magnitude predicted by SRIM

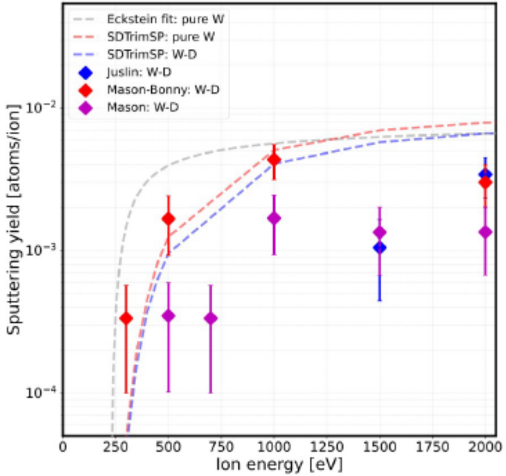

Potential	Formalism	Main purpose
Juslin	Tersoff	Modeling non-equilibrium processes
Mason-Bonny	EAM	Modeling vacancy clusters / Binding of nanometric hydrogen–helium clusters
Mason	EAM	Simulating hydrogen isotope retention

Potential dependence of the sputtering

The results of the simulations are significantly dependent on the interatomic potential:

- **Mason-Bonny:** Highest total sputtering but no molecular yield
- **Juslin / Mason:** Lower total sputtering but with molecular yield

SP D.2 Production of Atomic/Molecular and Surface Data: VTT

A. Sand

D005

Preliminary analysis of energy available for ro-vibrational states of sputtered molecules

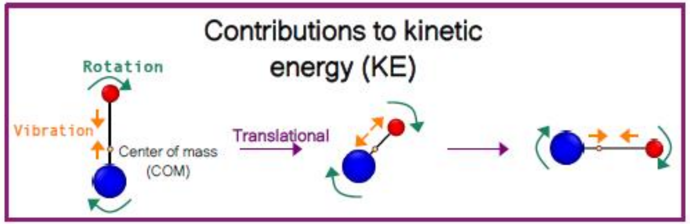

$$KE_{tot} = KE_{translational} + KE_{rotational} + KE_{vibrational}$$

$$KE_{tot} = KE_{atom\_1} + KE_{atom\_2}$$

$$KE_{translational} = \frac{1}{2} m_{tot} V_{com}^2$$

$$KE_{rotational} = \frac{1}{2} I\omega^2 = B_e J(J+1)$$

$$KE_{vibrational} = KE_{tot} - KE_{translational} - KE_{rotational} = h\nu_e \left(n + \frac{1}{2}\right)$$

From literature, if available
For D_2:
4401 cm^{-1} taken from NIST

$$B_e = \frac{h^2}{8\pi^2 \mu r^2}$$

- μ: reduced mass
- r: equilibrium bond length → taken from the potential

The "quantum numbers" obtained from the MD simulations are often not integer values, and they are rounded.

For D_2 molecules:

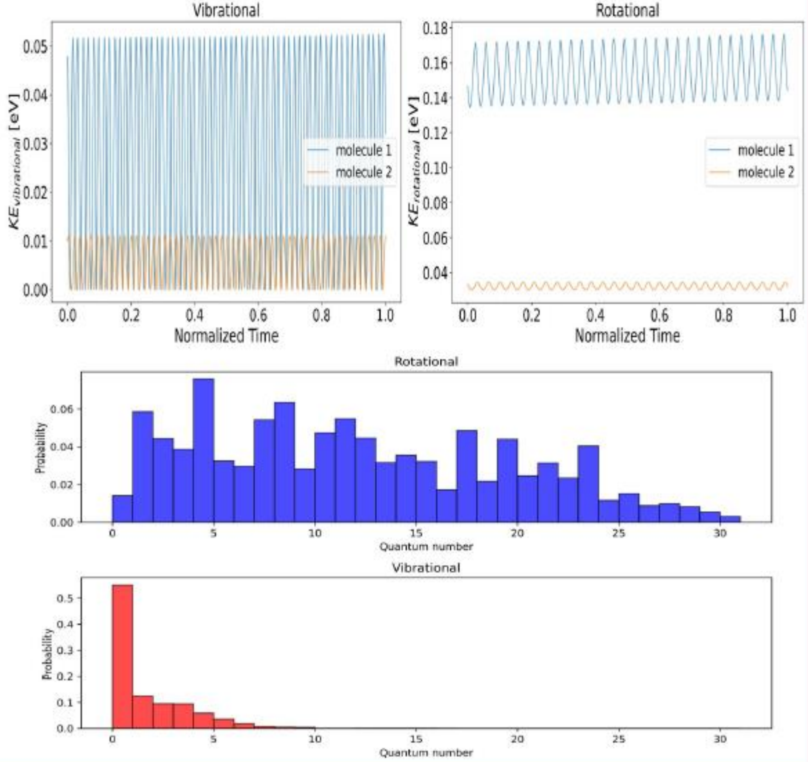

Effects of Surface Roughness on Particle Reflection

U. von Toussaint

D006

- **Reflection depends on roughness on nm-scale**

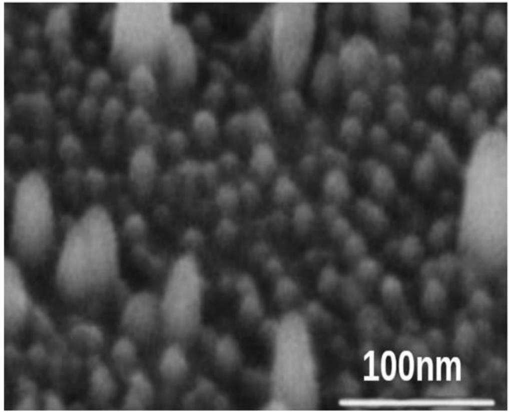

SEM-image: Roughening of Eurofer-sample under 200 eV D-irradiation [1]

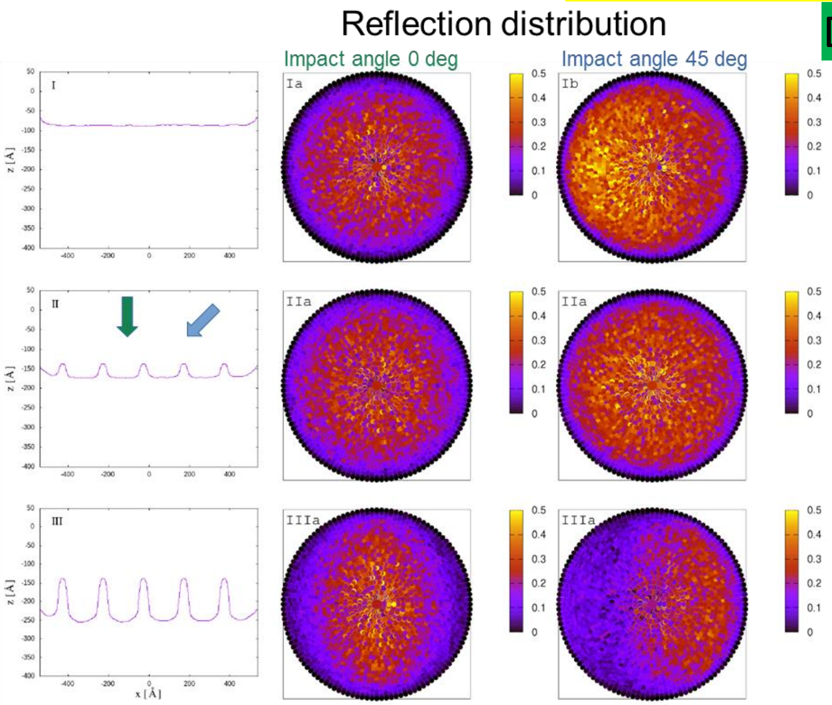

- Most PWI-codes (e.g. SOLPS, ERO) use reflection data based on assumption of atomistically flat surfaces
- Surface roughness may alter reflection distribution drastically (even momentum sign reversal → c.f. next slide)

Effects of Surface Roughness on Particle Reflection

U. von Toussaint

D006

SDTrimSP-2D : going beyond assumption of atomistically smooth surfaces (2024/2025)

SDTrimSP-7.0 : consider also sample crystallinity (2025)

- **Computation of 3-d reflection distributions**
- **(2 polar angles and reflection energy)**

- **Specular reflection strongly suppressed for**
- **light particles impinging on rough heavy target**
- **materials (ie. hydrogen isotopes on tungsten)**

- **Particle momentum parallel to surface may even**
- **be reversed by reflection at rough surfaces (cf graph)**

- **Effect more pronounced for shallower impact angles**
- **(as perpendicular impact has no parallel momentum)**

200 eV D on rough W (50 deg impact angle)

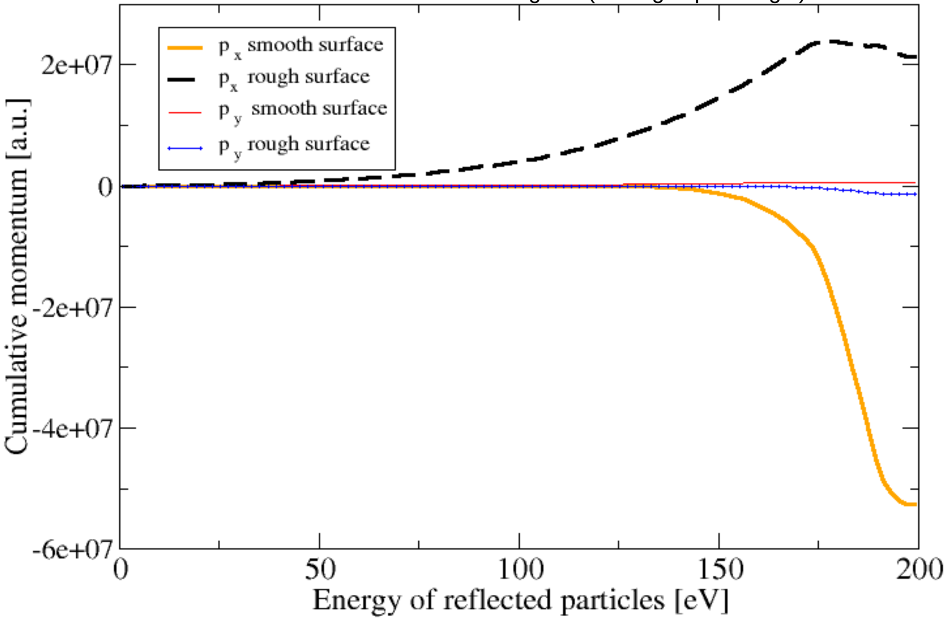

- **Simulation results supported by experimental results (although very sparse data basis)**

SP D.3 Impurity Migration Modelling

SP D.3 Impurity Migration Modelling: CEA

G. Ciraolo

D001

ERO2.0 modeling for WEST (focus on long-pulse, high fluence discharges)

→ **Few simulations with ERO2.0 using according plasma backgrounds seem to show better agreement with experimental erosion/deposition patterns**. More simulations required, work ongoing

ERO2.0 modeling of WEST discharges taking into account magnetic ripple

→ **ERO2.0 simulations started using 3D plasma background to study the impact on W sources, migration and core contamination**

SP D.3 Impurity Migration Modelling: ENEA

ERO2.0 microscale morphology studies

Dynamic helium retention

- Sputtering yields from SDTrimSP for W with He retained in surface (50%/50% composition, courtesy of FZJ) have been employed in ERO2.0 simulations
- Reduced net erosion and a better agreement with experimental effective sputtering yields

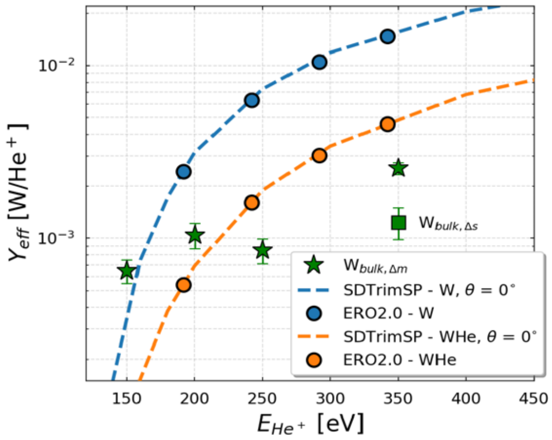

Crystalline orientation

- Sputtering yields from SDTrimSP7 relative to crystalline W with 110 preferential orientation provided, along with updated ones for amorphous W (courtesy of U. Von Toussaint and C. Baumann)
- Larger difference observed between old (SDTrimSP6, used in ERO2.0) and updated amorphous W yields than between updated amorphous and the crystalline yields, discussion ongoing on the use of these yields.

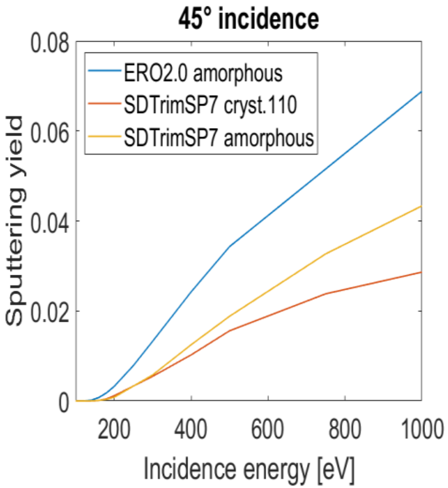

M. Passoni D002

SP D.3 Impurity Migration Modelling: ENEA

ERO2.0 global modelling in GyM

Objective: Perform preliminary simulations to support design of experiment aimed at studying W migration and deposition in GyM and validating global modelling.

Results:

- Experiment consists in mounting catchers on lateral wall bushings (fig.3) to catch W and Mo eroded from the sample-holder (SH) by He plasma and compare measured deposition to simulated one.
- Preliminary simulations investigated ideal position and orientation (ring-shaped catcher modelling, fig.4) of the catcher support.
- Results showed higher deposition closer to the SH and for orientations pointing towards the SH, placed at z = - 0.15m (fig.5 a-b).

(3)

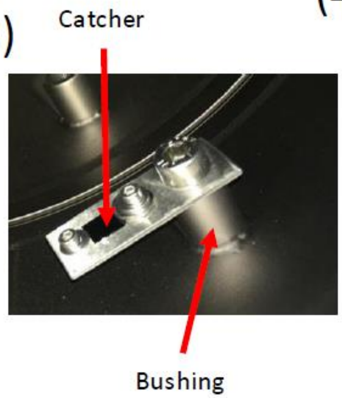

(4)

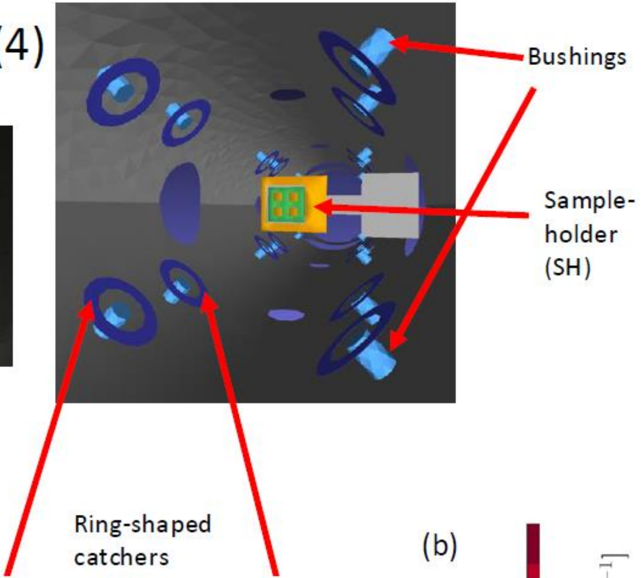

(5)

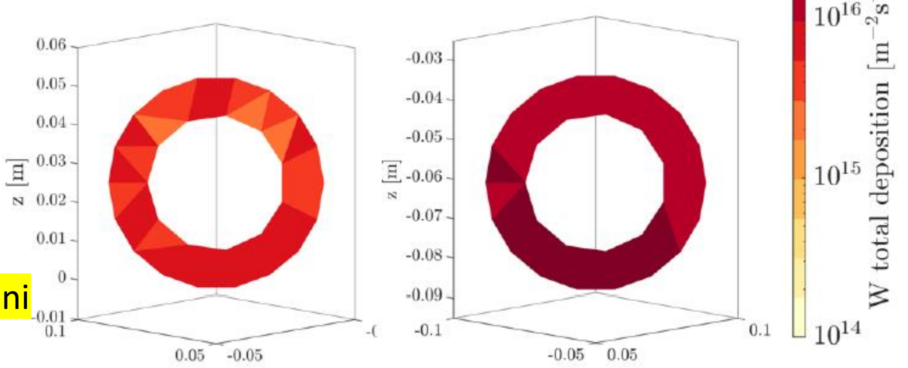

M. Passoni

D002

SP D.3 Impurity Migration Modelling: ENEA

M. Passoni

D002

ERO2.0 global modelling in AUG

Work is ongoing to produce H-mode He background plasma, under WP TE RT06, to be used as input for ERO2.0 simulations

SP D.3 Impurity Migration Modelling: FZJ

- ERO and ERO2.0 modelling of 13C injection experiments (local and global) in comparison to post-mortem data in W7-X and steady-state simulations.
  - Status: modelling of OP1.2 injection completed. (A. Kirschner, J. Romazanov)
  - Conference contributions:
    - A. Kirschner et al., ISHW 2024
    - A. Kirschner et al., EPS 2023
    - J. Romazanov et al., PSI 2024
  - Papers:
    - J. Romazanov et al., Nucl. Fusion (submitted 2024)
- ERO2.0 predictive modelling for full W environment in W7-X.
  - Status: ongoing, preliminary ERO2.0 simulations available. (J. Romazanov)
- ERO and ERO2.0 modelling of W prompt redeposition, in combination with sheath characteristics from PIC.
  - Status: ongoing, preliminary ERO simulations w/o PIC available, PIC profiles imported in ERO2.0 but no simulations yet. (A. Kirschner, C. Baumann)
- Initial simulations of ITER with full-W plasma-facing components and Ne seeding.
  - Status: ongoing, importing of plasma backgrounds and updated wall geometry in ERO2.0 ongoing (C. Baumann).

J. Romazanov, C. Baumann D003

SP D.3 Impurity Migration Modelling: FZJ

ERO modelling: Prompt W redeposition at inner ITER wall during ramping

A. Kirschner

D003

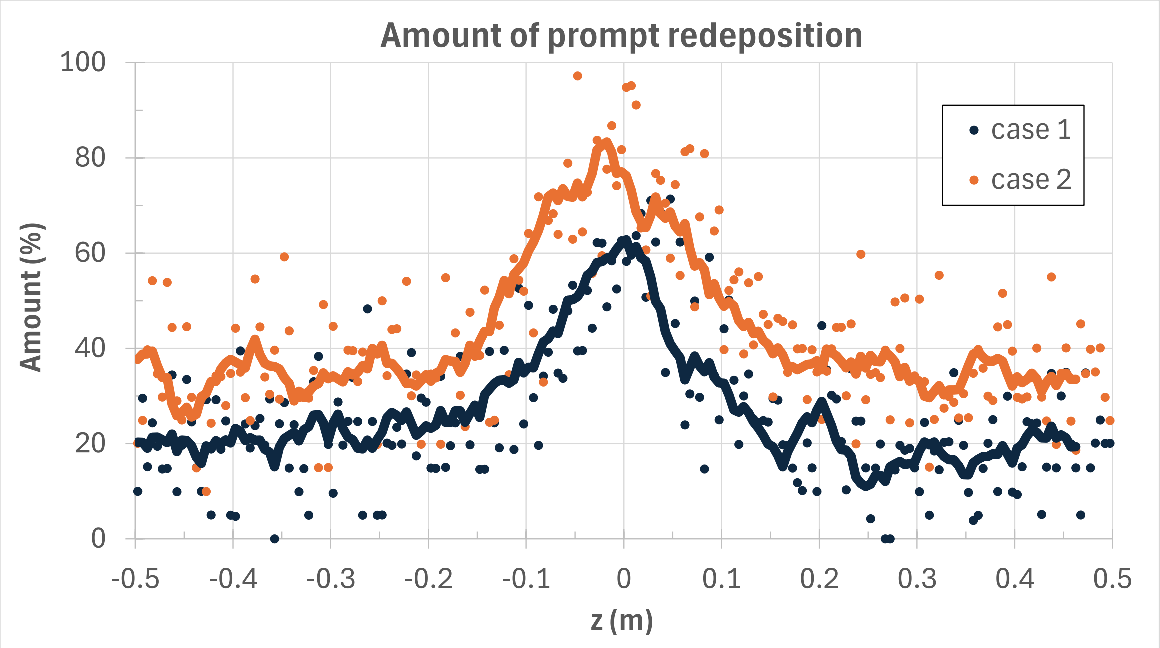

SOLPS-ITER background plasma provided by ITER IO for 2 cases:

case 1: 65 eV, 4e18 m^{-3}

case 2: 47 eV, 1e19 m^{-3}

W prompt redeposition fraction

- varies between 20% and 80%
- strongly depends on plasma parameter

SP D.3 Impurity Migration Modelling: MPG

WallDYN for ITER: W erosion rate depends on W-transport

K. Schmid

D004

- Depending on parallel (||-flows) and perpendicular $(D_{\perp}, v_{Pinch})$ transport the W charge state can exceed coronal equilibrium value at the wall
- ITER assumes very high far SOL temperatures

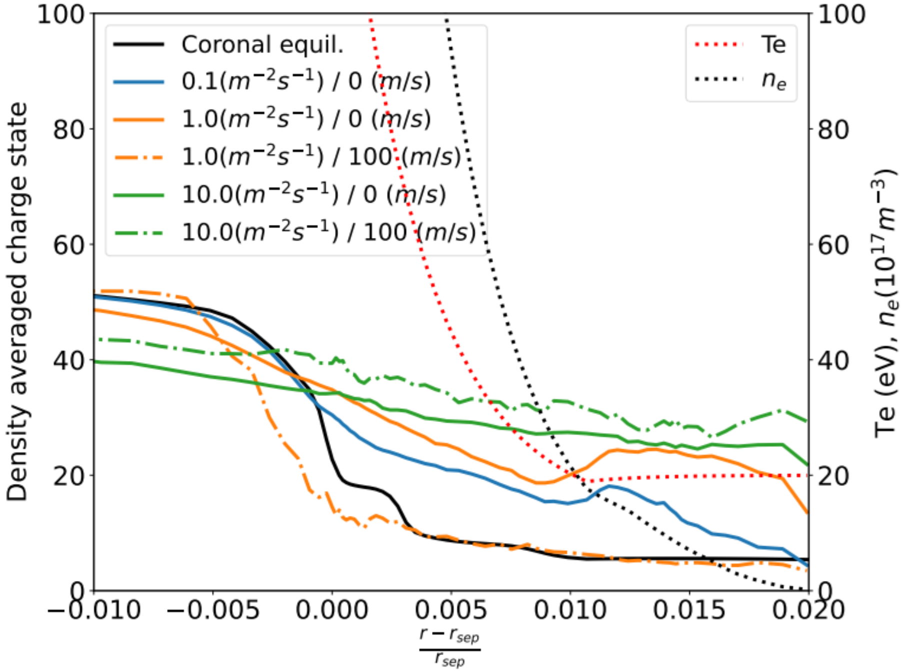

- High charge states + high T_e leads to strong sheath acceleration

→ Very high W impact energies at the wall

→ Y^{Self}>1

For $m_{i,i} \times \left(Y^{Self} + R^{Self}\right) \cong 1$ W erosion flux become infinite

$$\Gamma_W^{ERO} = \frac{\left(1 - m_{i,i} R^{Self}\right) \times \Gamma_{BKND}^{IN} \times Y^{BKND}}{1 - m_{i,i} \times \left(Y^{Self} + R^{Self}\right)}$$

SP D.3 Impurity Migration Modelling: MPG

WallDYN for ITER: why WallDYN predicts such high W erosion rates

K. Schmid

D004

❖ WallDYN computes the equilibrium influx Γ_W^{IN} of W onto each wall element by solving a linear equations system:

$$\Gamma_W^{ERO} = \underbrace{\Gamma_W^{IN} Y^{Self}}_{\text{Self-source}} + \underbrace{\Gamma_{BKND}^{IN} Y^{BKND}}_{\text{Bknd-source}}$$

$$\Gamma_W^{Ref} = \Gamma_W^{IN} R^{Self}$$

$$\Gamma_W^{IN} = m_{i,j} \times \left(\Gamma_W^{ERO} + \Gamma_W^{Ref}\right)$$

- The W erosion flux Γ_W^{ERO} corresponding to Γ_W^{IN} in reality is only reached **after many self-sputtering** generations
- The higher the self-sputtering enhancement of the primary erosion flux (wo. self-sputtering) the more generations are needed.
- Self-sputtering can enhance primary erosion by factors of 10 and more
- Primary erosion (Ne, D-CX, D+ only) is much lower

Case 2481 00g $D_\perp = 0.1\ m^2/s$

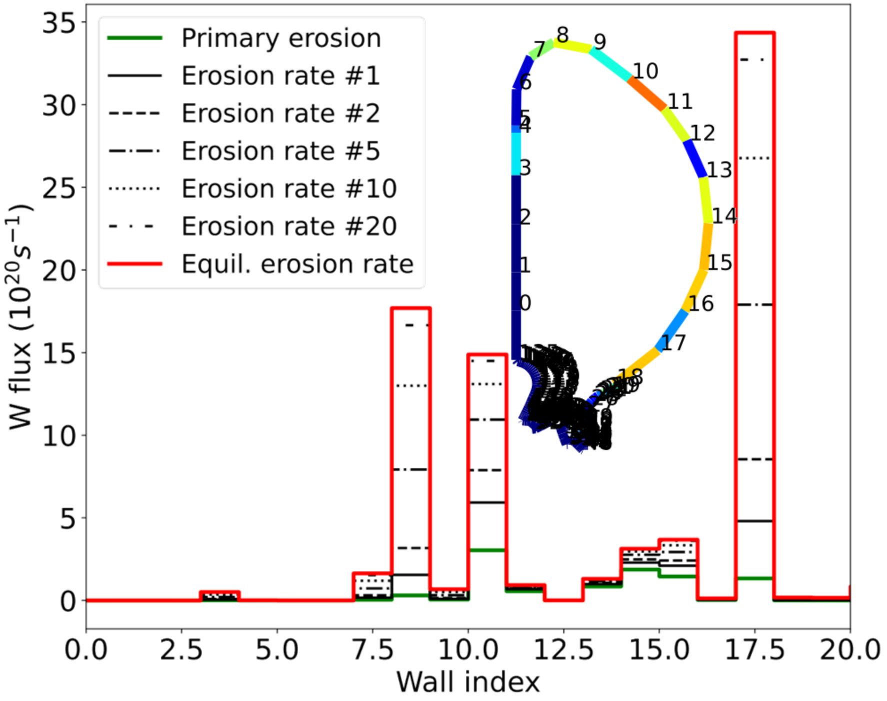

→ It takes more than 20 generation to reach equilibrium

SP D.3 Impurity Migration Modelling: MPG

WallDYN for ITER: boronization layer lifetime

K. Schmid

D004

- **Compute B re-erosion and transport in 3D using WallDYN3D with EMC3-Eirene for impurity transport**
  - Follow the erosion & migration from an initial 100 nm boronization layer on a W main chamber wall
  - Estimate the life time of such a layer for impurity gettering purposes

Surface concentration

- **Qualitative picture**

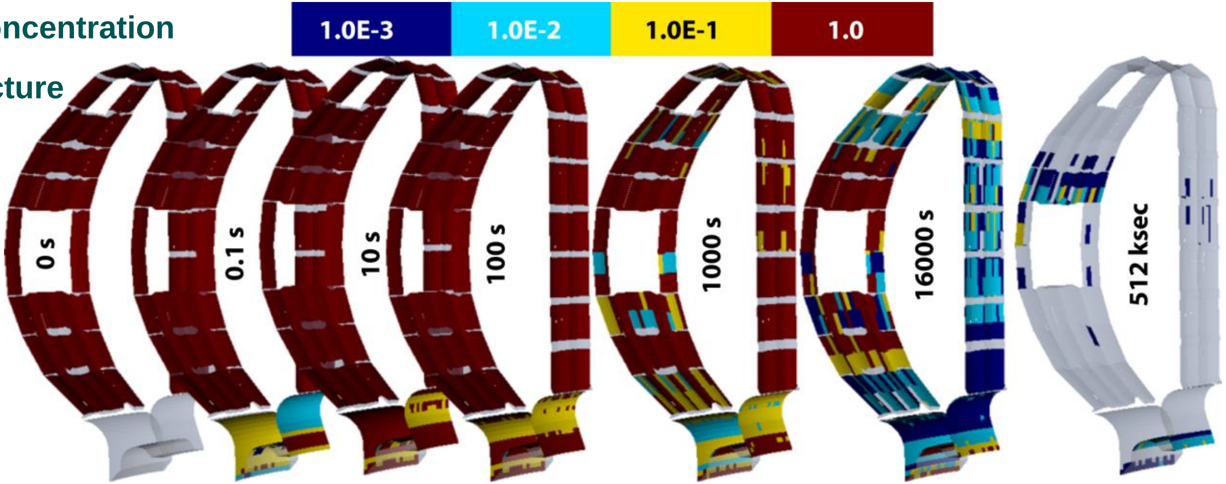

- Initially B deposits in divertor
- Plasma wetted areas are quickly eroded (O 1000s)
- As main chamber source depletes → deposition zones turn to erosion zones

- **Finally B ends up below inner divertor target**

SP D.3 Impurity Migration Modelling: VTT

Net erosion of Au markers in ASDEX Upgrade OSP region almost perfectly reproduced with ERO2.0

Implemented improvements in the simulation setup:

- Refined surface definitions
  - ⇒ Accurate sampling of BG plasma in PWI calculations of Au, Mo and W surfaces
- New background plasma from OSM
  - ⇒ Improved match to experimental divertor conditions
- Sputtering and reflection data for Au generated with SDTrimSP
  - ⇒ Physically representative sputtering yields to replace previously used Bohdansky formula estimates with no angular dependence

⇒ **Net erosion of Au primarily matched within 30% with experimental data in SOL**

- Deviation at OSP for the 1 × 1 mm² markers likely due to overestimated $n_{e,OSP}$ (no LP data at OSP) and experimental uncertainty of the OSP position

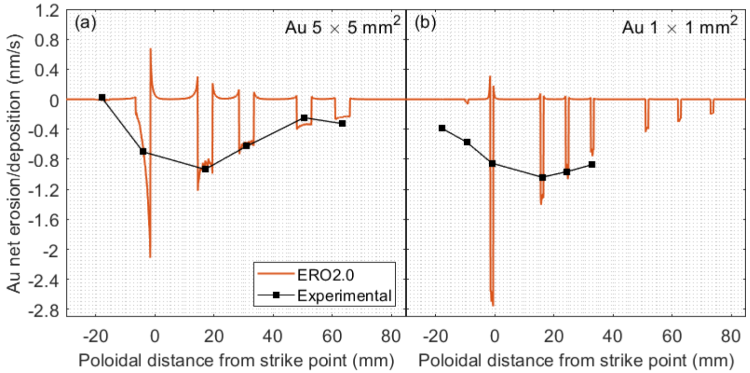

← Most significant source of improvement

Peak n_e likely exaggerated in lack of LP data

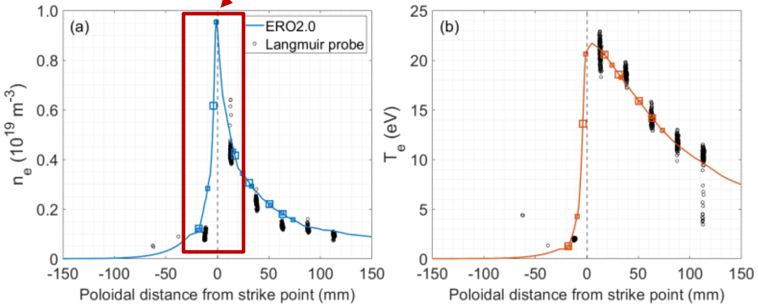

A. Hakola,
J. Karhunen, S. Saari

D005

SP D.3 Impurity Migration Modelling: VTT

Small Au markers found poor proxies for studying (particularly net) erosion of W PFCs

- Representativity of experimental setup assessed by
  - Comparing Au to W ⇒ effect of material choice
  - Comparing Au markers to toroidally extended Au surfaces ⇒ effect of geometry
- Gross erosion of Au 3—4 times stronger than for W due to higher sputtering yield
- Re-deposition of Au on **5 × 5 mm² markers** 2—3 times lower than on **toroidally extended Au surfaces** due to migration of eroded Au
- Unlike Au, W deposited also from BG plasma ⇒ further factor-of-2 effect on net erosion

⇒ **Net erosion of W surfaces overestimated by a factor of 15—20 by the 5 × 5 mm² Au markers**

W surfaces also changed to Au in simulations

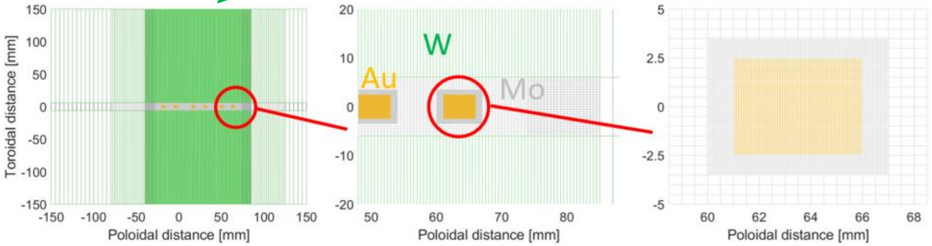

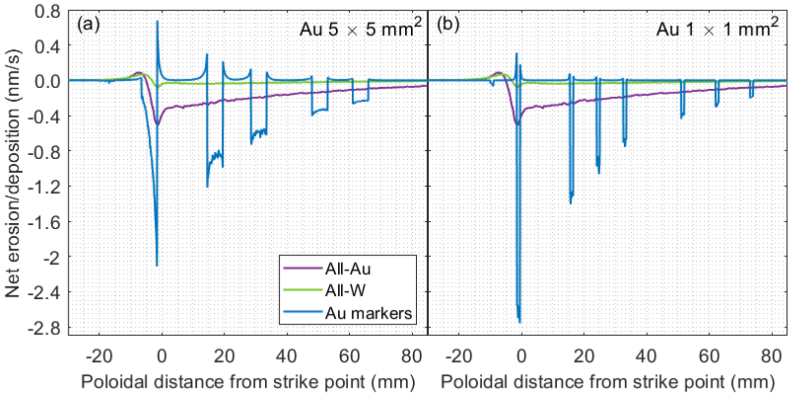

A. Hakola,
J. Karhunen, S. Saari

D005

SP D.3 Impurity Migration Modelling: VTT

M. Groth

D005

ERO2.0 modelling of Ni migration in JET

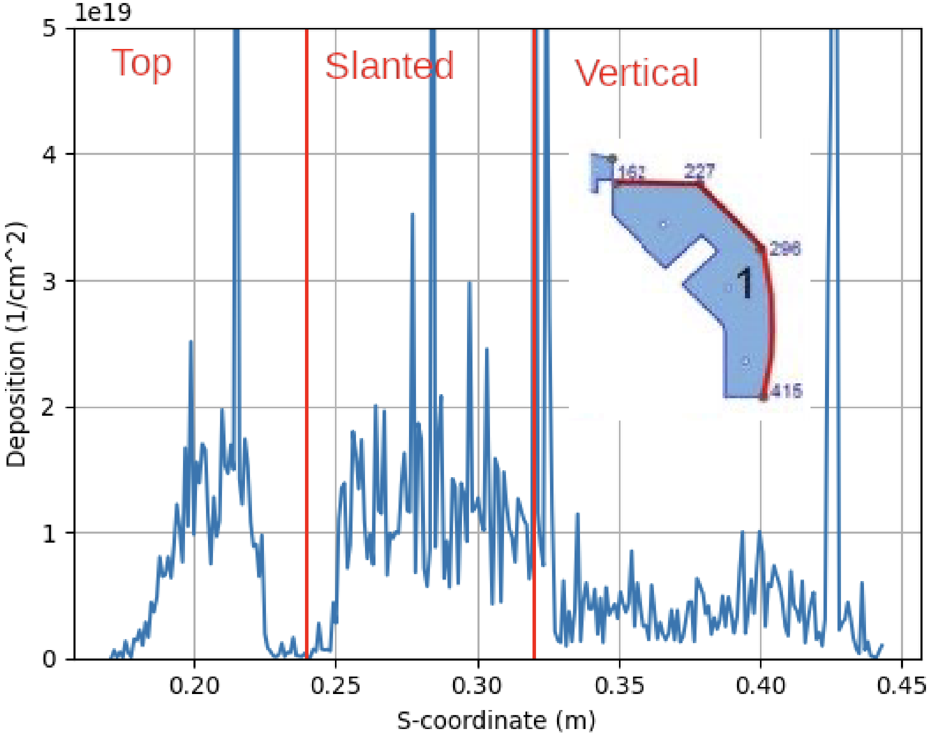

Predicted gross deposition of Ni onto tile: same order of magnitude as measured post-mortem

- EDGE2D-EIRENE to background plasmas (including flow) and CX atomic fluxes
- ERO2.0 to predict nickel erosion, transport and deposition in the JET-ITER-like-wall through years 2011-2016
- Primary erosion location on the vacuum vessel wall is predicted to be on the LFS near the midplane
- Nickel is transported onto the HFS divertor top ⇒ single deposition (no re-erosion yet assumed)

Boron dust adhesion

S. Ratynskaia

D006

- The non-retarded Hamaker constant of the boron-boron system was found to be $A_{BB} = 2.672 \times 10^{-19}$J. This is to be compared with $A_{WW} = 5.106 \times 10^{-19}$J for the tungsten-tungsten system. *Thus, the adhesive force of boron dust clusters should be expected to be half the adhesive force of tungsten dust clusters (of equal size).*

- The retarded Hamaker coefficient of the boron-boron system was also computed as a function of the separation until its reaches its asymptotic limit. It was successfully fitted to a theory-based analytical expression. The mean absolute relative error of the fit was merely 1.16%.

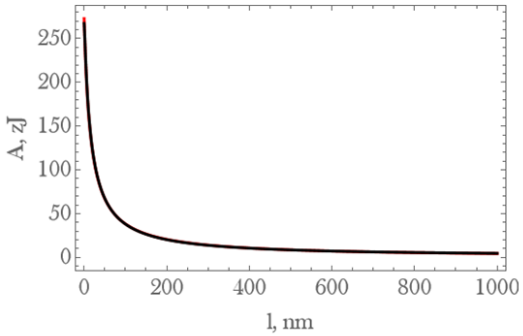

$$A_{BB}(l) = \frac{1}{0.00678 + 0.000417 \times l} + \frac{1}{0.00798 + 0.000487 \times l}$$

- The retarded Hamaker constant and the non-retarded Hamaker coefficient were also computed for the following fusion relevant combinations (where it is noted that boron nitride is anisotropic)
  - ✓ Boron – tungsten
  - ✓ Boron – boron nitride
  - ✓ Boron nitride – boron nitride
  - ✓ Boron nitride – tungsten

SP D.3 Impurity Migration Modelling: VR

Boron dust self-charging

S. Ratynskaia

D006

❑ MC simulations of electron transport inside boron carried out with the Geant4 software. Geant4 has four physics lists that are relevant for electron transport:

- ✓ Standard
- ✓ PENELOPE
- ✓ Livermore
- ✓ MicroElec

❑MicroElec is the most appropriate physics list for the modelling of tritiated dust self-charging due to beta decay. MicroElec utilizes Penn's algorithm for the implementation of linear response theory. We are currently implementing the boron optical ELF in MicroElec.

❑The most detailed study of tokamak dust self-charging was focused on tungsten and employed the EM-Opt4 package of Geant4 [Dougniaux *et al., J. Phys. Conf. Ser.* **1322**, 012027 (2019); Grisolia *et al., Nucl. Fusion* **59**, 086061 (2019)]. The study correctly sampled the experimental energy / angular distributions of internal beta electrons and utilized realistic tritium implantation profiles, but EM-Opt4 does not lead to accurate results for the secondary electron emission yield. Therefore, the calculated self-charging rates cannot be trusted.

SP D.4 Neutral Particles Modelling

SP D.4 Neutral Particles Modelling: KIT

DIVGAS: influence of the 3D geometric effects (e.g. poloidal and toroidal leakages) on the divertor performance for the DEMO baseline SN divertor case

Ch. Tantos, Th. Giegerich

D001

- The 3D simulation model is based on the latest DEMO 2020 divertor design (see Fig. 1) and includes one complete divertor sector (3 cassettes).
- We considered the following values for the inlet neutral pressure: P_{in}=1, 4, and 10 Pa, and the pumping probability: ξ=0.01, 0.1, and 0.3. – Such a range covers the plasma modelling prediction for the incoming pressure (≈4 Pa, provided by F. Subba) as well as the developed pumping technology for DEMO (DOI: *10.5445/IR/1000175884*).
- The poloidal gaps have a significant effect on the pumping efficiency. At low inlet pressures (P_{in}=1 Pa), about 7-10% of the incoming flux Φ_{in} returns to the plasma region through the poloidal gaps and reaches 12-18% for the high inlet pressure conditions (P_{in}=10 Pa).
- The effect of the toroidal gaps is weaker. It was found that about 1-3% of the incoming flux escapes through the toroidal gaps at the low inlet pressure scenario (P_{in}=1 Pa), and 2-8% at the high inlet pressure scenario (P_{in}=10 Pa).
- As the pumping probability decreases or the inlet pressure increases, the effect of the poloidal and toroidal gaps becomes more pronounced – This effect is more sensitive to the changes in the inlet pressure.

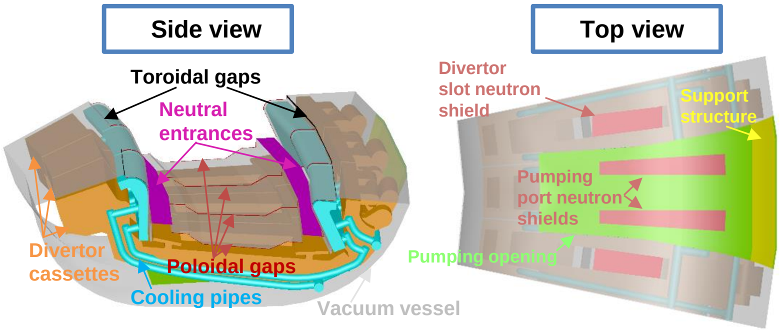

Fig. 1: 3D DEMO divertor simulation model.
IDM link: https://idm.euro-fusion.org/?uid=2PPMQB

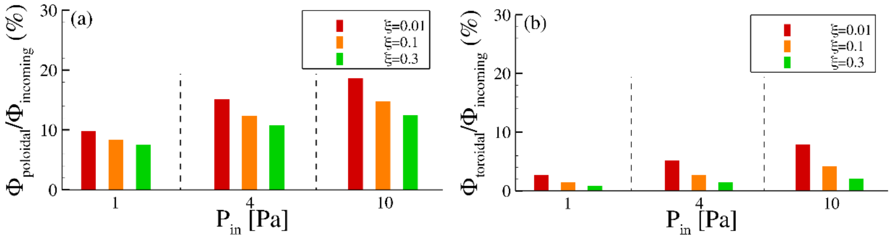

Fig. 2: Percentage of the total incoming flux that passes through poloidal gaps (a) and toroidal gaps (b) vs. pumping probability ξ.

SP D.4 Neutral Particles Modelling: KIT

DIVGAS: influence of the 3D geometric effects (e.g. poloidal and toroidal leakages) on the divertor performance for the DEMO baseline SN divertor case

Ch. Tantos,
Th. Giegerich

D001

- In the low inlet pressure scenario (P_{in}=1 Pa), approximately 2-10% (depending on the ξ) of the incoming flux is pumped out, while this percentage increases by a factor of 2 when the inlet pressure increases by a factor of 10 (see Fig. 3a).
- The highest percentage of the incoming flux returns to the plasma vessel through the entry gaps. In quantitative terms, this percentage is about 80-85% for P_{in}=1 Pa and about 60-70% for P_{in}=10 Pa (see Fig. 3b).
- The average pressure at the pumping opening varies between 0.05 Pa and 0.3 Pa for P_{in}=1 Pa and remains between 1.2 Pa to 5 Pa for P_{in}=10 Pa, with the low-pressure values always referring to the case of large pumping probability (see Fig. 4a).
- The pressure inside the divertor slot presents always the same behavior, i.e. high values in the area above the neutron shields and always low values in the area below them (see Fig. 4b). This decrease becomes more significant at large values of ξ and less significant at small values of ξ.
- The effect of neutron shields was also investigated. The results show that the presence of the neutron shields significantly affects the pumping performance (see Fig. 5a) resulting in a decrease of the pumped flux by about 30-40%.
- In contrast to the case with neutron shields (see Fig. 4b), the pressure inside the divertor slot varies slightly in the case without neutron shields (see Fig. 5b), with the greatest pressure drop being observed near the divertor entrances.

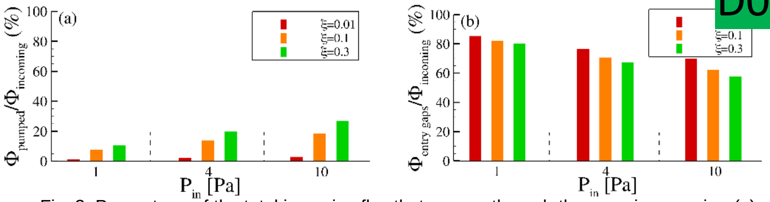

Fig. 3: Percentage of the total incoming flux that passes through the pumping opening (a) and entry gaps (b) vs. pumping probability ξ.

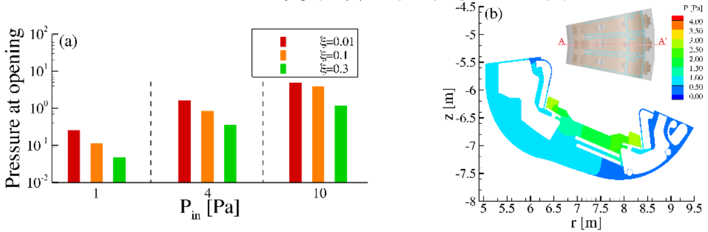

Fig. 4: a) Average pressure at the pumping opening vs. pumping probability ξ; b) Pressure contour for P_{in}=4 Pa and ξ=0.3 in the case with neutron shields along the vertical cross section A-A'.

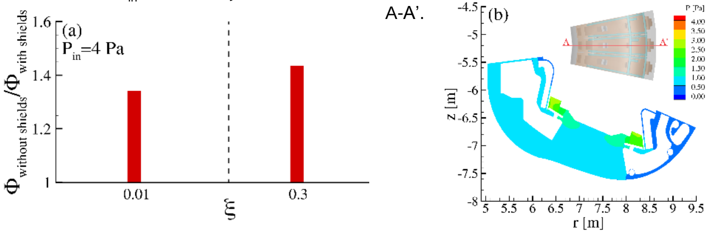

Energy-resolved CX fluxes to the wall predicted by EIRENE

M. Groth

D002

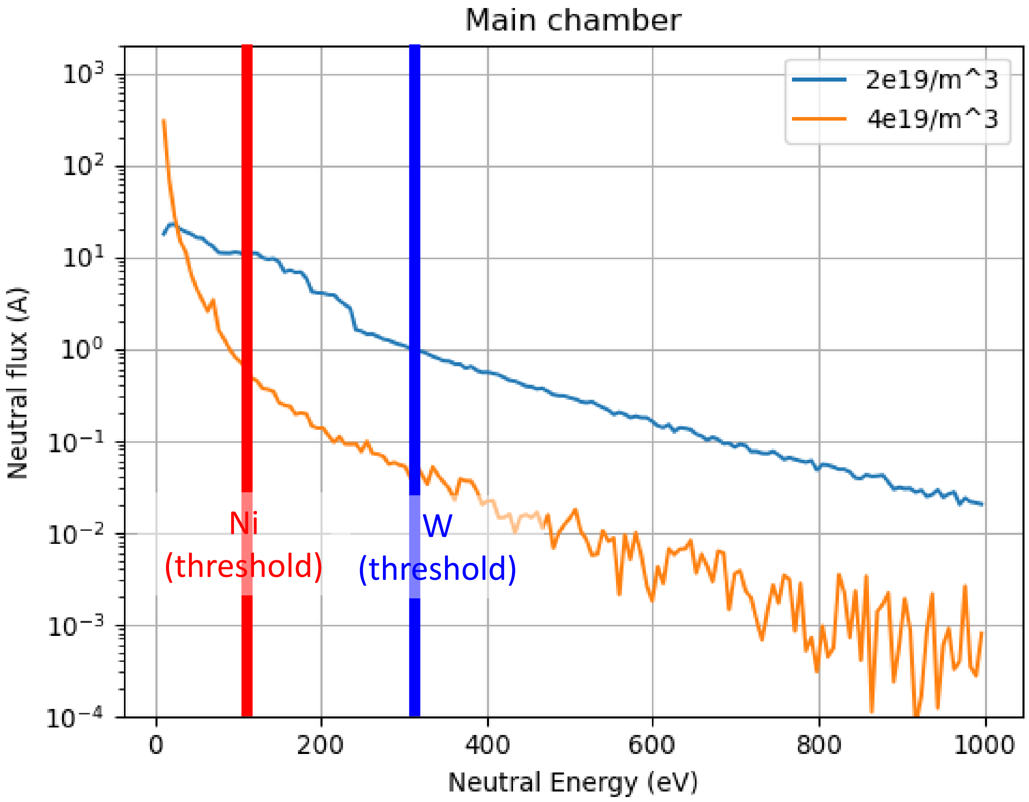

raising the core plasma density by 2x, EIRENE predicts up to 50x lower high-energy CX atoms

SP D.5 Plasma background and PWI Modelling for COMPASS-U

SP D.5 Plasma background and PWI Modelling for COMPASS-U: IPP.CR

D. Tskhakaya

D001

Plasma background modeling for COMPASS-U

- The new code version **SOLPS-ITER 3.2.0 Wide Grid**, has been successfully installed.
- First modelling of the **scenario #5400** has been performed: equilibrium, the B2.5 mesh has been built and an optimal conditions for the run have been found.
- Due to unavailability of Gateway, we expect some delay in simulations of the scenario #24300

Scenario (high performance H-mode, #5400)	
Toroidal magnetic field, Bt [T]	4.98
Plasma current, Ip [MA]	1.6
Total input power, Pinp [MW]	6.76
Core radiation, Prad [MW]	2.06
Total input power in SOL, Psol [MW]	4.7
Ion density in pedestal, n_i [m^{-3}]	$2.0*10^{20}$
Pure D discharges No impurities No drifts No currents	

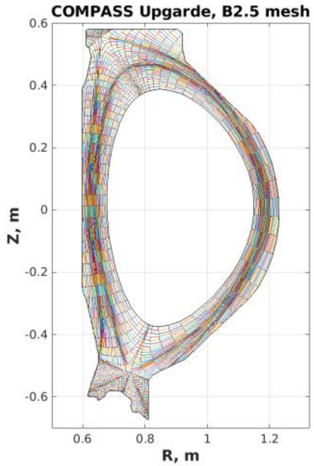

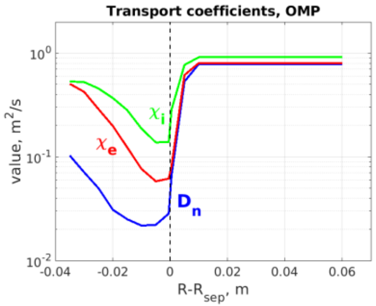

Simulation results

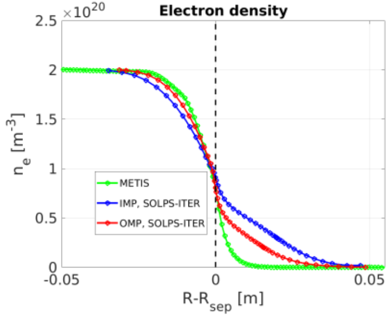

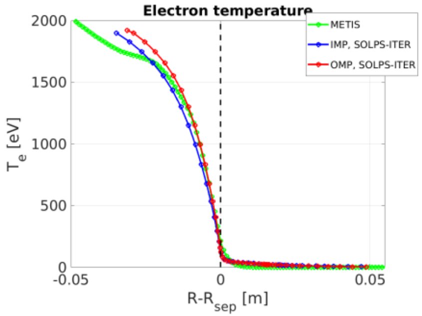

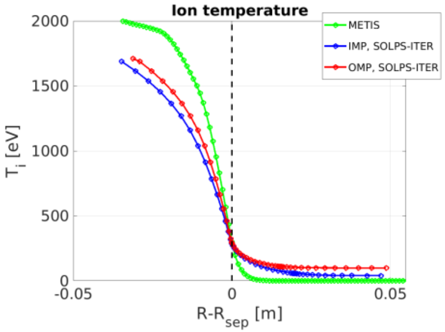

SOLPS-ITER simulation petameters were optimized to match separatrix and pedestal density and temperatures from core modelling code METIS. For the SOL the control parameter was λ_q.

To be noted that unphysically high ion temperature observed in simulations with the previous version of the code is not present in the new simulations.

SP D.5 Plasma background and PWI Modelling for COMPASS-U: IPP.CR

Preparation of ERO2.0 for simulations with W

- **Plasma background profiles from SOLPS**

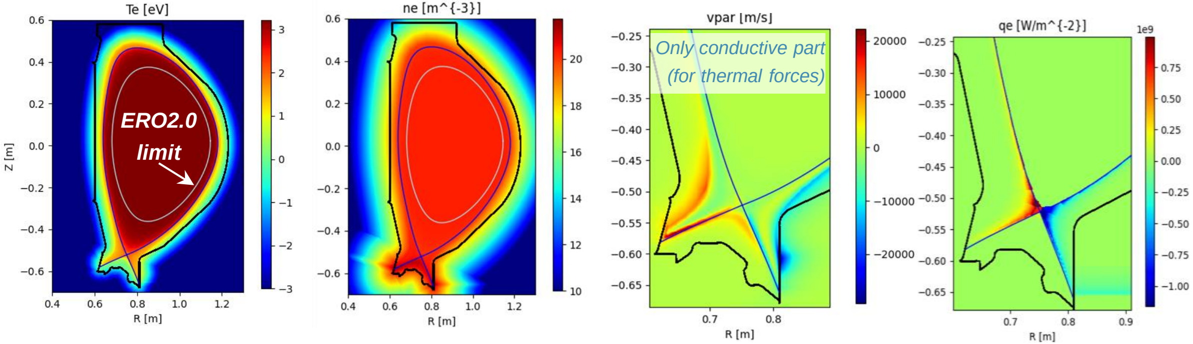

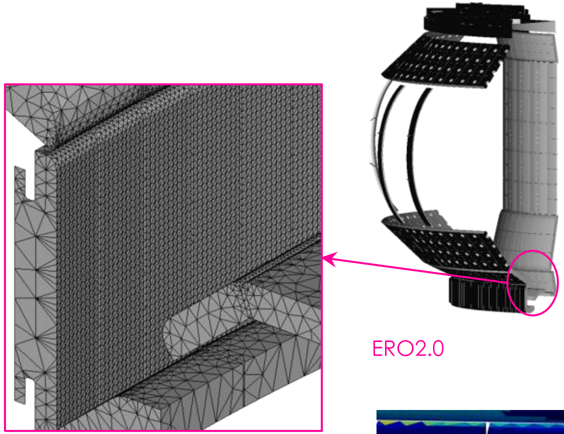

- **W transport coefficients from the FACIT code**

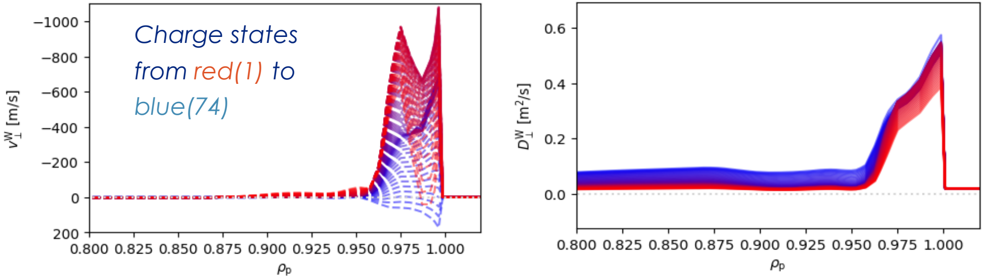

- **Shadowing patterns**

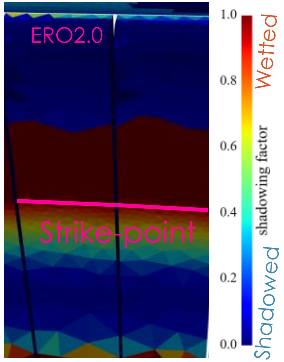

D. Tskhakaya D001

PIC simulations of the COMPASS-U SOL and divertor sheath

D. Tskhakaya

D001

- **Two sets** of simulations have been completed: high performance H-mode scenario #5400 and low density SOL. **No impurity** seeding.
- The **plasma sheath** in high density discharge seem to be **collisional** with subsonic plasma flow.
- Although the plasma is **detached** ($T_{e,div}$ ~3 and 7 eV), the **heat load** to the divertor is still **large** (see the table below)

	#5400 (ID / OD)	**Low n_e (ID / OD)**
$M_{\|\|}$ at the sheath entrance	0.45 / 0.45	1.0 / 1.0
Divertor heat load [MW/m^2]	**25.4 / 68.0**	5.3 / 10.1
W gross sputtering [$1/m^2$]	6.0×10^{19} / 10.0×10^{20}	5.3×10^{19} / 5.6×10^{20}
W prompt redeposition [%]	33 / 50	100 / 78

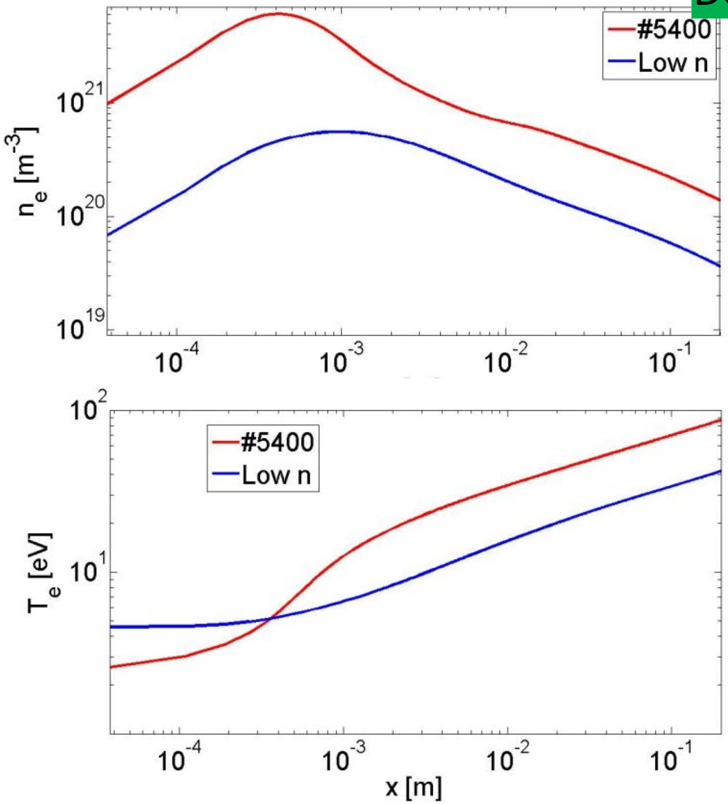

SP D.5 Plasma background and PWI Modelling for COMPASS-U: CEA

- Objective: produce SOLEDGE3X up-to-the-wall backgrounds for COMPASS-U and compare with SOLPS-ITER solutions
  - mesh and input files produced, running first test simulations

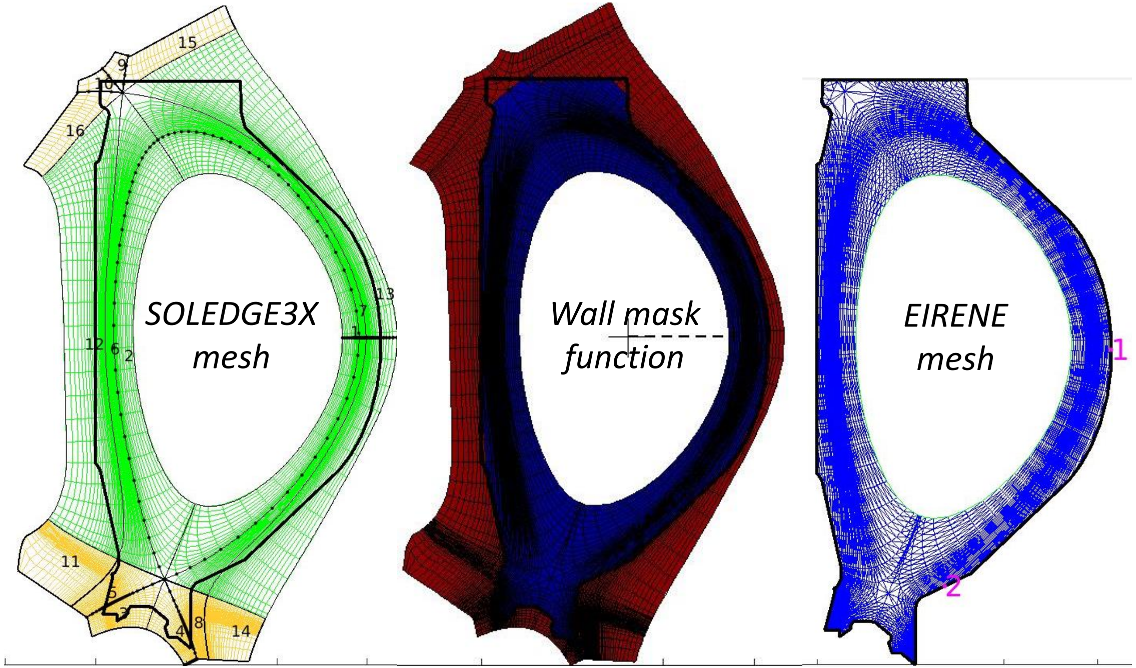

P. Tamain D002

Thank you very much for your patience !!!